Ore Geology Reviews 90 (2017) 772–789

Contents lists available at ScienceDirect

Ore Geology Reviews

journal homepage: www.elsevier.com/locate/oregeo

Contrasting mineralogical and processing potential of two mineralization types in the platinum group element and Ni-bearing Kapalagulu Intrusion, western Tanzania

Louis J. Cabri *, Harry R. Wilhelmij, Jacobus J. Eksteen

Cabri Consulting Inc., 700-702 Bank Street, PO Box 14087, Ottawa, Ontario K1S 3V0, Canada
Consulting Geologist, 3 Norham End, North Oxford OX2 6SG, England, United Kingdom[1]
Department of Metallurgical and Mining Engineering, Western Australian School of Mines, Curtin University, GPO Box U1987, Perth, WA 6845, Australia

ARTICLE INFO

Article history:
Received 2 November 2016
Received in revised form 3 April 2017
Accepted 6 April 2017
Available online 9 April 2017

Keywords:
Kapalagulu Intrusion
Laterite
Harzburgite
Platinum group mineralogy
Metallurgy

ABSTRACT

The Kapalagulu layered ultramafic and mafic intrusion is emplaced between the Paleoproterozoic Ubendian basement and overlying Neoproterozoic Itiaso Group metasedimentary rocks, located near the western shore of Lake Tanganyika. High-grade platinum group element (PGE) mineralization (1–6 g/t Pt + Pd + Au) is associated with chromitite and sulfide-bearing harzburgite within the southeastern extension of the intrusion, known as the Lubalisi Zone, which is covered by a layer of nickel-rich (0.2–2% Ni) laterite regolith that contains linear areas of PGE mineralization.

In the Lubalisi Zone, the mineralization may be divided into several significant geometallurgical domains: (a) high-grade PGE mineralization (1–6 g/t Pt + Pd + Au) associated with stratiform PGE reefs and chromitite seams within a harzburgite unit; (b) high-grade PGE mineralization (up to 12 g/t Pt + Pd + Au) associated with small bodies and veins of nickel massive sulfide within harzburgite below PGE-bearing reefs and chromitite seams; (c) low-grade PGE mineralization (0.1–0.5 g/t Pt + Pd + Au) associated with a sulfide-mineralized harzburgite unit above the PGE-bearing reefs; (d) laterite style residual PGE mineralization (0.2–4 g/t Pt + Pd + Au) associated with chromite concentrations in the saprolite and overlying red clay horizons of the laterite regolith; and (e) supergene Ni associated with the saprock and overlying saprolite clay.

Mineralogical study of three samples from the PGE reef consisting of high grade PGE chromitite and harzburgite indicate that this mineralization will give a good metallurgical response to conventional grinding and floatation due to the relatively coarse-grained nature of the PGM (P80 from ~37 to 52 μm), association with base metal sulfides, and unaltered gangue minerals (Wilhelmij and Cabri, 2016). In contrast, mineralogical and metallurgical study of the Ni and PGE mineralized laterite indicate that it cannot be processed using conventional mineral processing techniques but that a hydrometallurgical route should be used to recover the base and precious metals. Because any process is very much deposit-controlled, significant metallurgical and geometallurgical testing of mineralized samples, as well as pilot plant testing, will be required to arrive at feasibility studies.

© 2017 Elsevier B.V. All rights reserved.

1. Introduction

Since the discovery of low-grade copper and nickel mineralization on the western shore of Lake Tanganyika in the early 20th century, there have been intermittent field evaluations for Ni and Cu sulfide mineralization by many mining and exploration companies culminating in the discovery by BHP Minerals of platinum mineralization in a trench, which returned over 10 g/t PGE, associated with chromitite-bearing harzburgite and nickel-rich laterite in the 1990's. This exploration triggered a number of geological studies (e.g., Van Zyl, 1956, 1959; Wadsworth et al., 1982; Maier et al., 2007, 2008; Kasiri, 2005; Mbasha, 2007; Cabri et al., 2015; Wilhelmij and Cabri, 2016). From 2001 to 2009 Goldstream Mining, in Joint Venture with Lonmin PLC, explored for platinum and nickel in both the laterite and the harzburgite protolith in the southeastern dike-like extension of the Kapalagulu Intrusion known as the Lubalisi Zone as first reported by Wilhelmij and Joseph (2004).

* Corresponding author at: Cabri Consulting Inc., 700-702 Bank Street, PO Box 14087, Ottawa, Ontario K1S 3V0, Canada.
E-mail address: lcabri@sympatico.ca (L.J. Cabri).
[1] Formerly Lonmin-Goldstream JV, Australia.

http://dx.doi.org/10.1016/j.oregeorev.2017.04.009
0169-1368/© 2017 Elsevier B.V. All rights reserved.

This paper reports new findings from mineralogical and metallurgical work undertaken in 2004–2005 (Wilhelmij and Wilhelmij, 2004, 2005, 2006; Cabri, 2004a, 2004b, 2004c). The rationale is to prioritize new approaches for metallurgical characterization of PGE-bearing harzburgite reefs and associated laterite based on mineralogy, and existing or experimental metallurgical processing options. Mineralogical results from pristine PGE-bearing harzburgite indicate that the PGM can be recovered by conventional milling and floatation circuits that are used to recover PGM and base metal sulfides from the Upper Group Number 2 (UG2) Chromitite and Merensky Reef of the Bushveld Complex and the Main Sulfide Zone of the Great Dike (Cawthorn, 2002, 2015; Prendergast, 1988). Mineralogical studies from the PGE-bearing laterite show that various metallurgical scenarios should be considered for PGE (and Co, Ni) recovery. Due to the remote location, size of the deposit and capital investment required, smelting of concentrates produced at site may prove to be uneconomic. Becker et al. (2014) indicated flotation of weathered and oxidized ores often leads to poor flotation recoveries if smeltable grades are targeted. In Becker's study, the highest 4E PGE flotation recovery obtained was 39%. The highest Pt recovery was 52%, and the highest Pd recovery was 20%. These recoveries were obtained despite sodium bisulfide (NaSH) preconditioning to enhance flotation. This highlights the significant risk to a flotation-based recovery process for PGE minerals from oxidized and weathered ores.

Direct leach approaches are therefore considered to be more appropriate. Mpinga et al. (2015) reviewed various direct leach approaches to PGE extraction. Most approaches discussed involve a two stage process where the base metals (Ni, Cu, Co) and most of the iron and sulfur are removed prior to extraction of the PGE's. This limits the reagent consumption associated with PGE extraction which normally require more expensive lixiviants than sulfuric acid with strong complex-forming properties.

The challenges of effluent disposal also need to be taken into account since hydrometallurgical processing routinely consumes significant quantities of reagents (which might not be fully recovered), generate large quantities of aqueous effluents, leach residues and precipitates (e.g. gypsum, jarosite, goethite and/or hematite). Water consumption from the Lubalisi River or Lake Tanganyika and solid waste disposal are other important considerations for hydrometallurgy. This paper explores the interactions among the geology and mineralogy in arriving at metallurgical processing options.

2. Geological setting of Kapalagulu Intrusion

The Kapalagulu Intrusion is a 30 km long and up to 3 km wide dike-like layered igneous body (lopolith) located at the foot of an escarpment that forms part of the eastern rifted margin to Lake Tanganyika in western Tanzania. This intrusion is one of a series of mafic and ultramafic intrusions that stretch from northern Tanzania across Burundi into western Tanzania, that are known as the Central African Nickel Belt (cf., Duchesne et al., 2004; Maier et al., 2008). The Central African Nickel Belt intrusions were emplaced into the Mesoproterozoic Kibaran orogenic belt (1100–1400 Ma) and the Paleoproterozoic Ubendian Belt basement (older than 1800 Ma) and have an age of about 1400 Ma (Deblond et al., 2001; Maier et al., 2007). These intrusions are composed of medium-to-large layered mafic and ultramafic bodies, small magma conduits (chonoliths and sills) and dike swarms (Evans et al., 2016). The location of the Kapalagulu Intrusion with respect to the major tectonic domains of Tanzania and neighboring countries is shown in Fig. 1.

The northwest trending dike-like Kapalagulu Intrusion is subdivided into two domains: A northwestern domain of well layered gabbroic rocks exposed on the side of an escarpment capped by Mesoproterozoic metasediments; and a southeastern domain of poorly layered dunite and harzburgite buried beneath a thick laterite regolith that forms an undulating plateau below the escarpment. The two contrasting lithological sequences present in the domains are known as the Lower Ultramafic Sequence (3100 m thick) and the Upper Mafic Sequence (1350 m thick) (Van Zyl, 1956, 1959; Wadsworth et al., 1982; Wilhelmij and Joseph, 2004; Wilhelmij and Cabri, 2016; Maier et al., 2008).

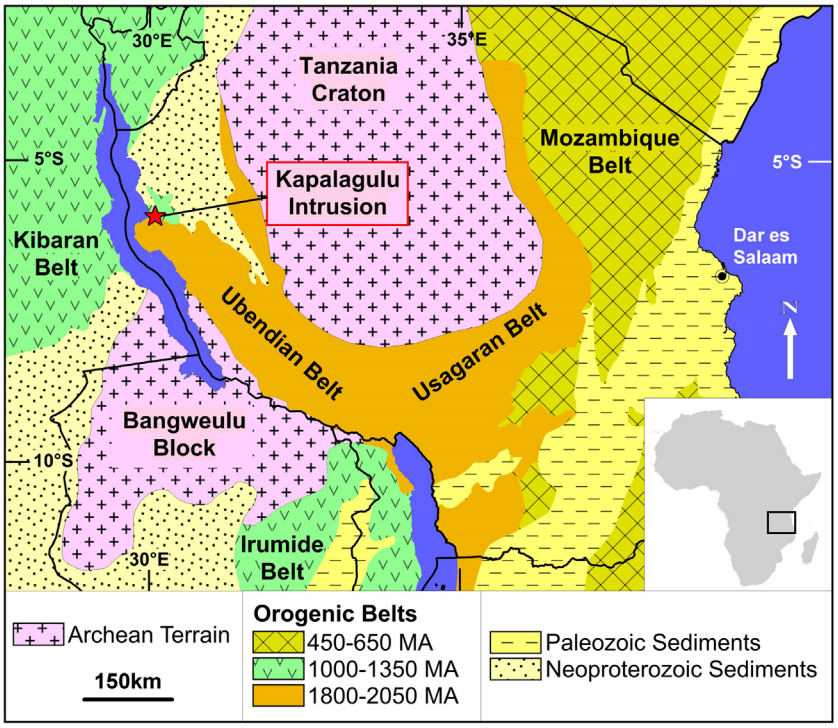

Fig. 1. Location of the Kapalagulu Intrusion with respect to the geology of Tanzania.

The structure of the Lower Ultramafic Sequence forms a tight syncline that plunges to the northwest and has been extensively modified by axial parallel faults. This synclinal structure which is bounded by the Ubendian Belt basement gneiss, is known as the Lubalisi Zone and has been the focus of extensive exploration and resource drilling for magmatic and lateritic Cu, Ni and PGE mineralization.

3. PGE mineralization in the Lubalisi Zone harzburgite

In the Lubalisi Zone of the Kapalagulu Intrusion the Lower Ultramafic Sequence consists of a Basal Dunite (270 m thick), Lower Feldspathic Harzburgite (330 m thick), the Main Chromite Sulfide Succession (130 m thick; MCSS), Sulfide Harzburgite (200 m thick), Upper Harzburgite (390 m thick) and Layered Harzburgite and Troctolite (240 m thick) (Wilhelmij and Cabri, 2016). Diamond drilling of the various harzburgite stratigraphic units has identified stratiform PGE mineralization in thin intervals (reefs) of chromite and sulfide enrichment near the base of the Lower Feldspathic Harzburgite, and within the harzburgite of the MCSS. Drilling has also identified small massive sulfide bodies, rich in Cu, Ni and PGE, in the Lower Feldspathic Harzburgite below the PGE reefs of the MCSS and widespread low grade PGE mineralization associated with the Sulfide Harzburgite that overlies the MCSS (Wilhelmij and Joseph, 2004).

The Lubalisi PGE-bearing reefs have similarities with the Merensky Reef and PGE-bearing chromitite layers (e.g. UG2) of the Bushveld Complex of South Africa (Cawthorn, 2002, 2015). The Lubalisi reefs differ from the PGE-bearing Main Sulfide Zone of the Great Dike of Zimbabwe by the presence of abundant chromite and olivine, and absence of vertical offset styles of Pt and Pd enrichment (Prendergast, 1988).

A simplified structural cross section through the Lubalisi Zone (Fig. 2) outlines the synclinal geometry of the layered dunite and harzburgite and the stratigraphic location of the PGE reef-bearing MCSS. Also shown in Fig. 2 is the Sulfide Harzburgite stratigraphic unit that overlies the MCSS and contains widespread low grade PGE mineralization associated with disseminated sulfides. The PGE reefs of the MCSS are described in detail by Wilhelmij and Cabri (2016); they are impersistent along strike and are in places stacked vertically. These PGE reefs can be subdivided into the following three groups depending on the presence or absence of visible chromite or sulfide: (1) Chromitite seams and bands, (2) Chromite- and sulfide-bearing harzburgite, and (3) Sulfide harzburgite with minor chromite. In the various chromitite seams and bands of the chromite-bearing harzburgite, there is invariably fine to very fine-grained sulfide that can be identified with a hand lens.

Four drill core samples were taken from PGE reefs intersected in the KPD24 and KPD44 drill holes (see assays in Table 1 of Wilhelmij and Cabri, 2016; locations shown in Fig. 2) for PGM analysis and the results are discussed in Wilhelmij and Cabri (2016) and in later sections.

4. PGE and Ni mineralization in the Lubalisi Zone laterite

The Lower Ultramafic Sequence of the Kapalagulu Intrusion within the Lubalisi Zone is covered by an up to 20 m thick interval of laterite regolith (Fig. A1). Consequently, the harzburgite that dominates the Lubalisi Zone is only exposed along the Lubalisi River and associated tributaries that have eroded into the laterite surface. Results from the widespread drilling of the laterite shows that the high-grade areas of PGE (>1 g/t Pt + Pd + Au) and Ni (>0.8%) are associated with the underlying harzburgite bedrock that contain varying concentrations of sulfide and chromite. This mineralized harzburgite is associated with the Main Chromite Sulfide Succession (MCSS), containing PGE reefs, and the overlying Sulfide Harzburgite, both of which dip away (in synclinal fold limbs) from the Ubendian Belt basement contacts. The spatial distribution of the areas of higher grade Ni and PGE laterite are shown in Fig. 2 and clearly outline the synclinal structural geometry of the mineralized harzburgite bedrock within the Lubalisi synclinal structure.

The laterite regolith of the Lubalisi Zone is described by Wilhelmij and Cabri (2016). It consists mostly of oxides of Fe and Al and from the weathered saprock upwards, is composed of four lithostratigraphic horizons, these being saprolite clay, ferruginous red clay (ferralite), pisolitic ferricrete (duricrust) and red laterite soil (Fig. A1). These horizons can inter-finger with each other and thickness varies according to topography. Geochemically, they represent an accumulation of Fe_2O_3 and Al_2O_3 and a partial to total loss of SiO_2 and MgO. It is important to note that the horizons differ from each other in color, grain size, density and chemical content.

Drilling of closely-spaced vertical holes through the laterite along traverses across the Lubalisi Zone show that it is possible to trace the PGE reefs within the MCSS lithostratigraphic unit up dip into the laterite profile, where there are residual concentrations of chromite and PGE in the saprolite and/or the ferruginous red clay horizons of the laterite regolith. A schematic diagram illustrating the progressive laterite deflation and weathering of the PGE reefs over time is shown in Fig. 3.

Closely-spaced drilling allowed calculation of inferred mineral resource estimates for the laterite mineralization using different cut-offs and were the rationale for PGM analyses and metallurgical testwork. Resources using Ni cut-offs are: at 0.5% Ni envelope 113.1 million tonnes of 0.82% Ni, 0.05% Co and 0.1% Cu; at 0.8% Ni envelope 49.5 million tonnes of 1.06% Ni, 0.06% Co and 0.12% Cu. Resources using Pt + Pd + Au cut-offs are: at 0.5 g/t envelope 22.7 million tonnes of 0.87 g/t Pt + Pd + Au and 0.9% Ni; at 1 g/t envelope 5.5 million tonnes of 1.52 g/t Pt + Pd + Au and 0.97% Ni; at 1.5 g/t envelope 1.8 million tonnes of 2.15 g/t Pt + Pd + Au and 1% Ni; at 2.0 g/t 0.9 million tonnes of 2.72 g/t Pt + Pd + Au and 1% Ni (Gotley, 2005; Armstrong, 2005).

Base metal distribution in the laterite regolith cross-sections of Fig. 4 show that the Ni mineralization, with isolated domains of associated Cu mineralization, is concentrated in the saprolite clay and at the interface of the clay and saprock. The Ni and Cu concentrations represent supergene mineralization associated with laterite chemical weathering. Precious metal distribution in the laterite regolith cross-sections of Fig. 4 show that the Pt + Pd + Au mineralization is coincident with Cr mineralization. This represents residual PGM mineralization associated with chromite derived from the in-situ laterite weathering of PGE reefs and chromitite seams (Fig. 3).

A detailed illustration of the vertical base and precious metal assays (Table A2) in the laterite intersected in the two PGE-rich metallurgical drill holes (KPD91 and 92) is shown in the assay line graphs of Fig. 5. The PGE-rich laterite intersections from the two drill holes represent the residual remnants of two separate PGE reefs within the MCSS harzburgite that are inclined to the southwest. The down-hole metal distribution line graphs show that there is a significant downward supergene Ni enrichment in the saprolite clay overlying the harzburgite saprock and that the Pt, Pd and Rh values mimic that of the Cr peak concentrations in the saprolite clay, implying in-situ residual concentration during the lateritic weathering of PGE reefs and associated chromitite seams. There is some supergene Au and Cu mineralization associated with the saprock and overlying saprolite clay Ni-enrichment.

In conclusion, there are two large scale geometallurgical domains within the Lubalisi laterite regolith, the supergene Ni associated with the saprock and overlying saprolite clay and the residual PGE and chromite in the saprolite and overlying red clay.

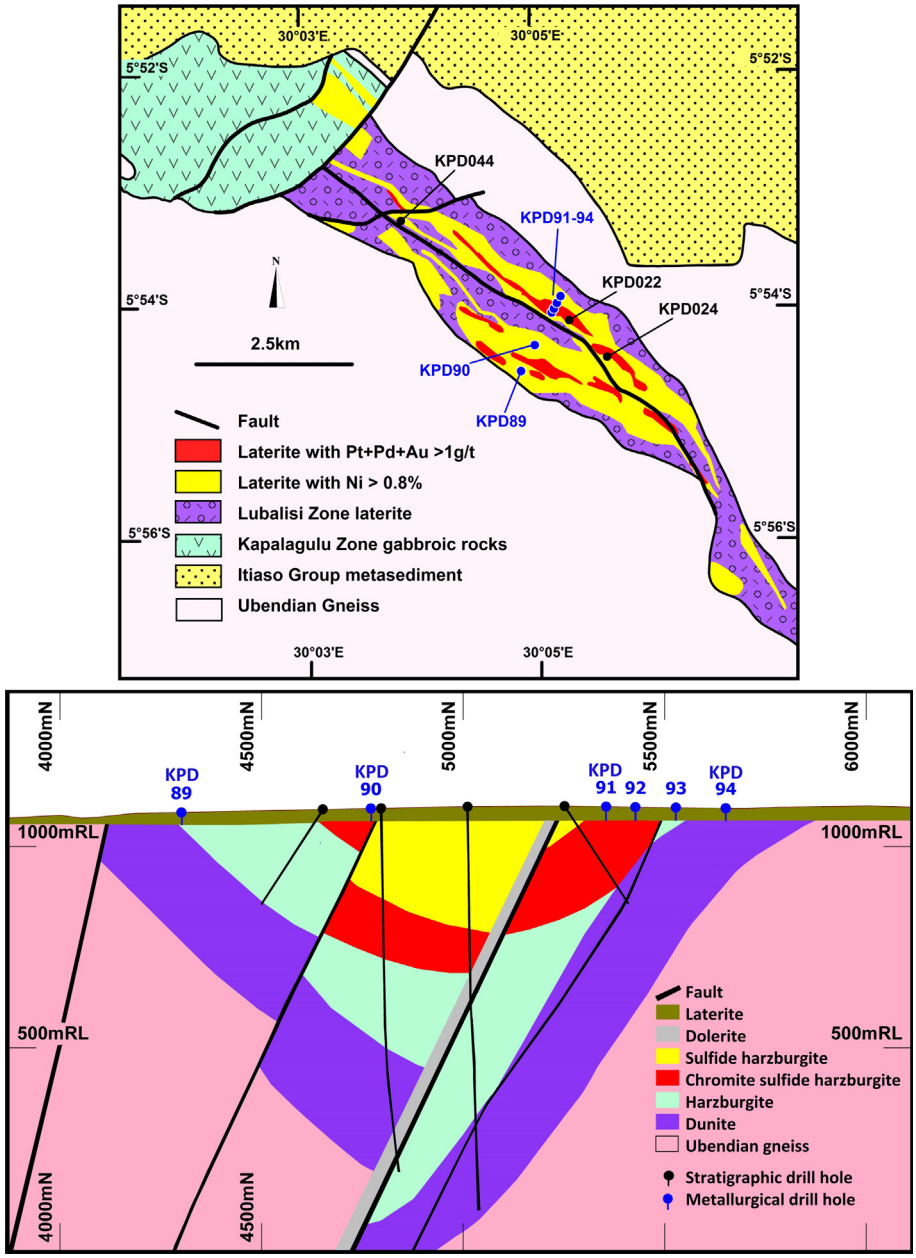

Fig. 2. Top: Simplified geology map of the Lubalisi Zone showing laterite nickel and PGE resource areas with respect to the drill holes from which mineralogical and metallurgical samples were taken. Bottom: Cross-section of the Lubalisi Zone showing the location of the metallurgical laterite drill holes in relationship to the underlying harzburgite stratigraphy.

5. PGE geometallurgical domains

Significant resources of PGE mineralization in the Lubalisi Zone are associated with the PGE reefs and chromitite seams within the MCSS harzburgite lithostratigraphic unit and the weathered expression of this bedrock mineralization in the covering laterite regolith (Fig. 4). There is other high grade PGE mineralization associated with small Ni massive sulfide bodies and thin veins in the Feldspathic Harzburgite unit below the MCSS. There is also low grade PGE mineralization associated with the Sulfide Harzburgite unit above the MCSS.

In summary, four significant PGE-rich geometallurgical domains in the Kapalagulu Intrusion have been identified:

i. High grade PGE (up to 12 g/t Pt + Pd + Au) associated with small bodies and veins of Ni massive sulfide present below the PGE reefs and chromitite seams (not investigated in this study).
ii. High grade PGE (1–6 g/t Pt + Pd + Au) associated with PGE reefs and chromitite seams within the MCSS harzburgite unit.
iii. Low grade PGE (0.1–0.5 g/t Pt + Pd + Au) associated with the Sulfide Harzburgite lithostratigraphic unit above the PGE reefs (not investigated in this study).
iv. Residual PGE (0.2–4 g/t Pt + Pd + Au) associated with chromite concentrations in the saprolite and red clay horizons of the laterite regolith.

There is most likely a fifth PGE geometallurgical domain that is associated with the supergene laterite Ni (contact between the saprolite clay and the harzburgite saprock), which has related supergene Pd, Au and Cu enrichment, but this domain is not clearly

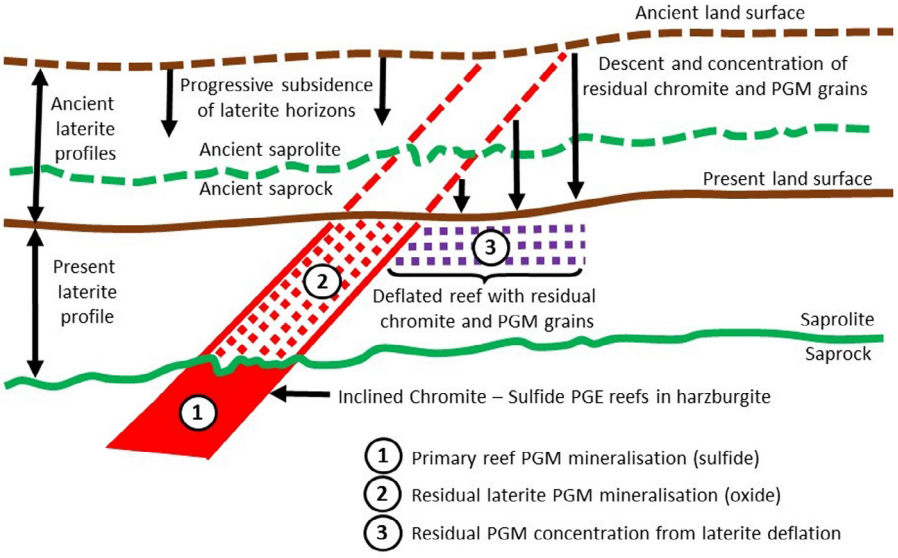

Fig. 3. Schematic diagram showing vertical subsidence of the Lubalisi laterite landscape through inclined Chromite–PGE reef layers. There is progressive disintegration of the PGE reefs during descent of the laterite surface over time.

defined by the present drill hole lithological logging and sample assay data.

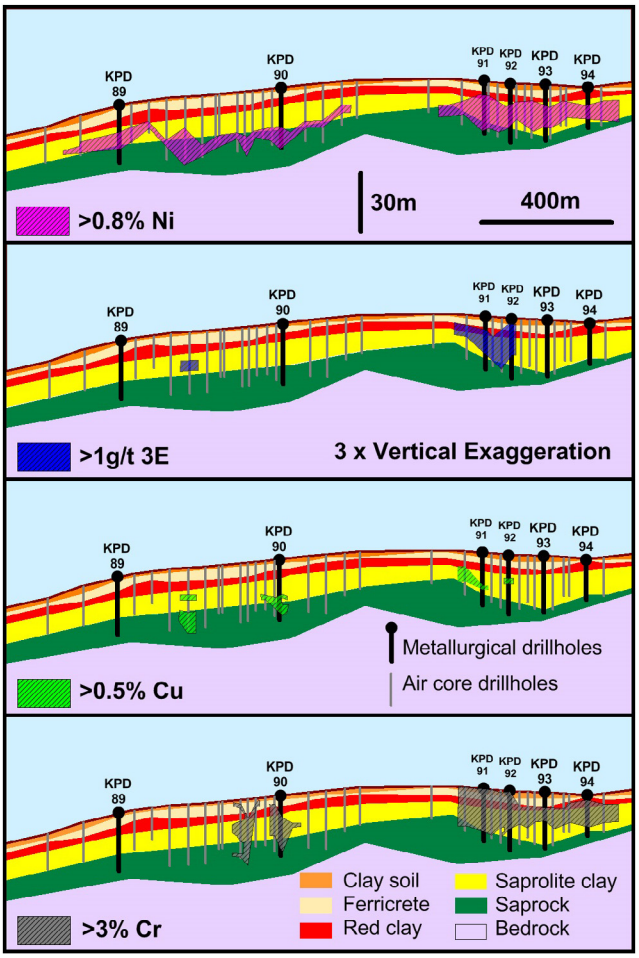

Fig. 4. Stacked cross-sections showing the metallurgical drill holes in relationship to the PGE, Ni, Cr, and Cu resource domains in the laterite regolith.

Mineralogical investigations have focused on two of the geometallurgical domains: the PGE reefs and chromitite seams and the associated PGE mineralized laterite saprolite clay. Metallurgical investigations have focused on the PGE laterite geometallurgical domain as the mineralogical study on the PGE reefs with chromite seams geometallurgical domain indicates that this domain may be processed using conventional Bushveld Complex-style flotation, smelting, and base and precious metal refining.

6. Materials and methods

The samples studied mineralogically consisted of four diamond drill-core samples from two different diamond drill holes (KPD44 and KPD24) in chromite-sulfide harzburgite and five samples from drill hole KPD22 in the laterite regolith, ranging from ferricrete near the surface to saprolite at the base. Details of assay, sample preparation, and techniques used are described in detail by Wilhelmij and Cabri (2016) and may be summarized as follows. PGE reef samples were examined as polished thin sections by ore microscopy; the remainder of each sample was studied by X-ray diffraction, Scanning Electron Microscopic (SEM) and electron microprobe techniques. High-grade heavy mineral concentrates were made from crushed and sized drill core by hydroseparation (e.g., Cabri, 2004d; Cabri et al., 2005) to quantify the mineralogy (modal analyses of the major/minor minerals, grain-size analysis, and liberation characteristics of the minerals as in Lastra et al. (1998) and to search for and characterize platinum-group minerals (PGM) and gold minerals (see Wilhelmij and Cabri, 2016 for details).

To study the precious metal mineralogy, the oxidized lateritic samples (KPD22) were first subjected to attrition milling and the coarser "grit" fractions were then studied by similar techniques used for the PGE reef samples, except that no polished thin sections were prepared. The "clay" fraction was qualitatively studied by X-ray diffraction. A split of each of the oxidized samples with no attrition milling were coarsely crushed (<2 mm) and analyzed by image analysis. The results of this coarse crushing, as obtained by sieving, are shown in Fig. 6, and where it can be seen that fines were minimized as only from 19.4 to 32.8% of the particles are finer than 106 μm.

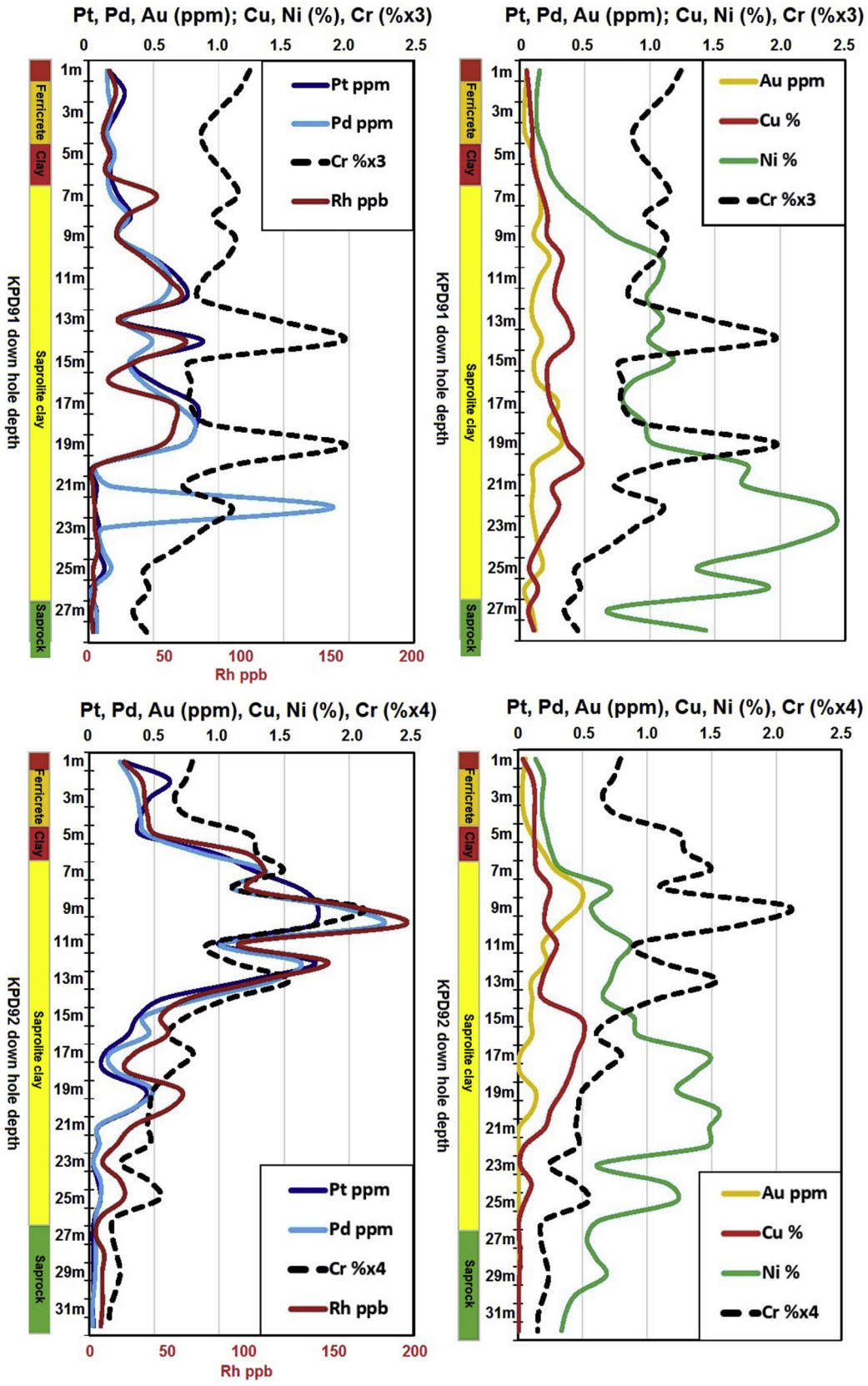

Fig. 5. Down-hole precious and base metal distributions for the two vertical metallurgical drill holes that penetrated PGE-rich lateritic regolith.

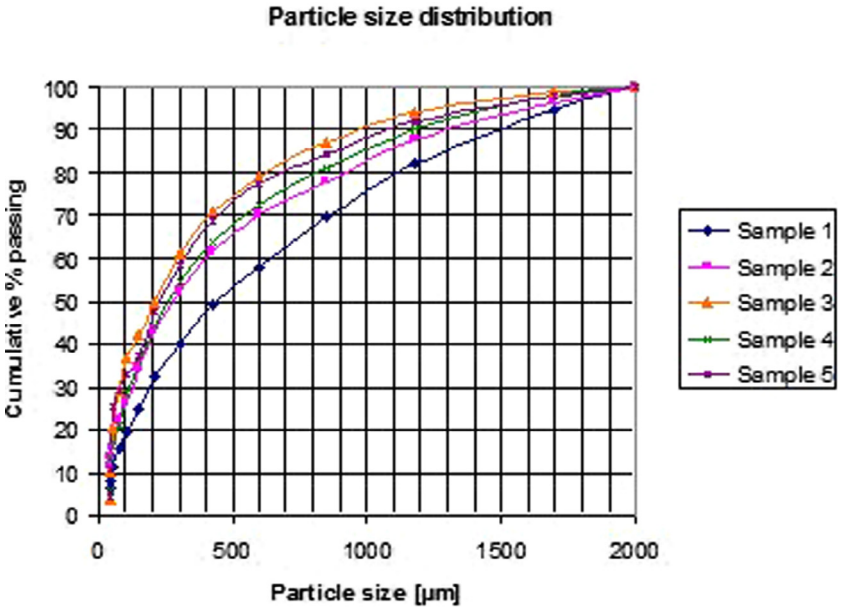

Fig. 6. Cumulative % passing size distribution of the five samples after coarse crushing.

7. Results

7.1. Assays for PGE reef and laterite samples

Assays for the PGE reef and the laterite samples that were studied geochemically are summarized in Table 1 and Table 2 of Wilhelmij and Cabri (2016). Metallurgical testwork by SGS Lakefield was done on selected laterite samples for which the mineralogy was not studied by assuming the mineralogy was similar to that reported for one drill hole (KPD22) by Cabri (2004c). The metallurgical testwork was completed on samples characterized by chemistry as ferricrete, low Mg saprolite (LoMgSAP), and high Mg saprolite (HiMgSAP). Size-by-size assays reported by SGS Lakefield are shown as calculated head concentrations in Table 1, which also includes data for Rh.

7.2. Gangue mineralogy of PGE reef samples

Quantitative image analyses reconciled to assays show that the principal minerals belong to the kaolinite-serpentine group [lizardite $Mg_2Si_2O_5(OH)_4$], the chlorite group [clinochlore $(Mg,Al)_6(Si,Al)_4O_{10}(OH)_8$], olivine ($Mg_2SiO_4$), pyroxene (enstatite $Mg_2Si_2O_6$), and chromite ($FeCr_2O_4$), with but minor to trace quantities of magnetite (Fe_3O_4), chalcopyrite ($CuFeS_2$), and pentlandite [$(Fe,Ni)_9S_8$], as listed in Table 2.

Particle size distributions for the four PGE reef samples after coarse crushing are given in Fig. 7. The grain size distributions to determine the predicted grind to liberate the minerals for the four PGE reef samples are shown graphically in Fig. A2. It is shown that liberation at the minimum grind (K80) is fairly coarse for chromite and magnetite (~87 to 91 μm), the sulfides are finer-grained: chalcopyrite (~25 μm), pentlandite and pyrrhotite (~16 to 18 μm). Liberation at the optimum grind (K40) is (~8 to 10 μm) for the three sulfides and ~44 to 46 μm for chromite.

7.3. Precious metal mineralogy of the PGE reef samples

Because there was insufficient material available for making high-grade concentrates for sample 081914 the searches for precious metal minerals were limited to the other three samples. A total of 364 precious metal minerals were identified and measured (summarized in Table 3) and details on the abundance by frequency and relative percent by mass are shown graphically in Fig. 8. The grain-size distributions for the PGM and gold minerals are shown graphically for samples D395 and D396 in Fig. 9, which demonstrate the significance of coarsest grains to the mass balance.

Analysis for trace Pd in pentlandite showed that it represents a significant proportion of the total Pd, ranging from 13.5% to 21.0% (Wilhelmij and Cabri, 2016). The association data show large proportions of free particles at the grind used and are summarized graphically in Fig. 10 and the grain size distributions for the precious metal minerals are given in Fig. 11.

7.4. Gangue mineralogy of laterite samples

The five oxidized samples from the laterite "clay" fraction were qualitatively analyzed by X-ray diffraction of "clay" and showed that goethite is abundant in all samples and that undifferentiated "magnetite-maghemite" is a minor component in all but sample

Table 1
Summary of assays of three samples for metallurgical testwork.

	Calculated head concentrations from size by size assays from SGS Lakefield data											Assays (heads)
Name	Al%	Co%	Cr%	Mg%	Ni%	Ag ppm	Au ppb	Pd ppb	Pt ppb	Rh ppb	4E* ppb	4E ppb
LoMgSAP PGE	7.09	0.14	4.05	1.16	0.86	1.4	193	944	1027	94	2257	2572
HiMgSAP PGE	3.25	0.05	1.39	4.52	1.10	1.0	96	326	292	37	752	741
Ferricrete	9.39	0.03	5.08	1.11	0.31	0.6	39	223	373	41	675	1696

* 4E = Pt + Pd + Au + Rh.

Table 2
Measured and calculated modal analyses of four PGE reef samples.

Minerals	D395		D396		081914[1]		010369	
	IA wt%	Assays wt%	IA wt%	Assays wt%	IA wt%	Assays wt%	IA wt%	Assays wt%
Mainly lizardite and clinochlore	43.0		55.0		24.0		22.8	
Forsterite and enstatite	28.1		31.3		49.1		48.8	
Minerals with higher atomic number than forsterite & less than chromite	0.02		0.08		0.01		0.03	
Chromite[2]	25.6	16.04	10.1	6.28	25.3	15.86	27.3	17.07
Magnetite	1.3		0.47		0.04		0.03	
Pyrrhotite	0.2	0.36	0.6	0.57	0.1	0.14	0.01	-0.34
Chalcopyrite	0.6	0.60	0.6	0.68	0.3	0.31	0.2	0.25
Lead[3] and PGM	0.01		0.13		0.07		0	
Pentlandite	1.2	1.34	1.2	1.38	1	1.07	0.8	0.94
Totals	100.0		99.5		99.9		100.0	

[1] There was not enough assayed S to correspond to the Ni and Cu as sulfides.
[2] The Cr % in chromite is quite variable (23–46%). The calculated chromite uses an average composition for %Cr. That may explain why calculated chromite is less than measured by image analysis (IA).
[3] The presence of some particles of native Pb were determined to be contamination during crushing; did not affect the results except this caused many more "bright" particles that had to be checked.

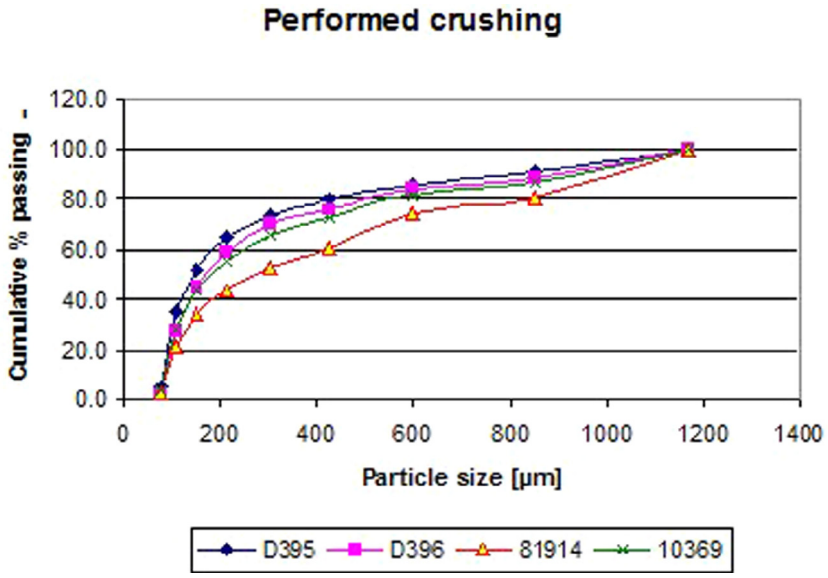

Fig. 7. Cumulative % passing size distribution for the PGE reef samples.

9550-2, where this is a major component (Wilhelmij and Cabri, 2016, Online Resource F6). Maghemite (Fe_2O_3, γ-Fe_2O_3) is formed by weathering or low-temperature oxidation of spinels containing ferrous iron. It has the same spinel ferrite structure as magnetite and is also ferromagnetic. All five samples were shown to be magnetic, varying from slightly (9550-1) through moderately (9550-5) to highly magnetic (9550-2–9550-4). Under the SEM, the distinction between goethite [ideally α-FeO(OH)] and hematite (ideally Fe_2O_3) was made on the basis of texture and composition. Hematite is usually pure iron oxide with little Al or Si and has a uniform appearance in backscattered mode and often has round bubble-like voids. The proportion of hematite drops substantially in the samples with increased depth. Goethite usually has significant Al and/or Si and is texturally complex, with obvious banding or botryoidal features and is a major component in all samples, although its habit changes as sample numbers increase with depth. The major minerals (chromite, hematite, and goethite) were analyzed (see Table 3 in Wilhelmij and Cabri, 2016).

Table 3
Grain sizes and abundance of PGM and Au minerals for three PGE reef samples (n = 364).

Sample	P80 (µm)	P50 (µm)	Number grains
D395	52	33	134
D396	40	25	93
10369	37	25	137

The modal analyses by image analysis of all five samples are given in Table 4 using analyzed mineral compositions when available, otherwise ideal or average compositions were used. Chromite is the main carrier of Cr but hematite, goethite, and clinochlore also carry some Cr. Assuming all the Cr is in chromite, the calculated amount of chromite from assays was used to assess the quality of the image analysis results (Table 5). It can be seen that the chromite quantity calculated using the average analyses by electron microprobe is comparable with the measured amount of chromite.

The grain size distributions to determine the predicted grind to liberate the minerals are shown graphically in Fig. A3. It is shown that liberation at the minimum grind (K80) for goethite (gt) increases from the top down to 9550-4, ranging from ~82 µm to ~134 µm before becoming very fine-grained in 9550-5 (~42 µm). In contrast, chromite (cr) is finer-grained but also

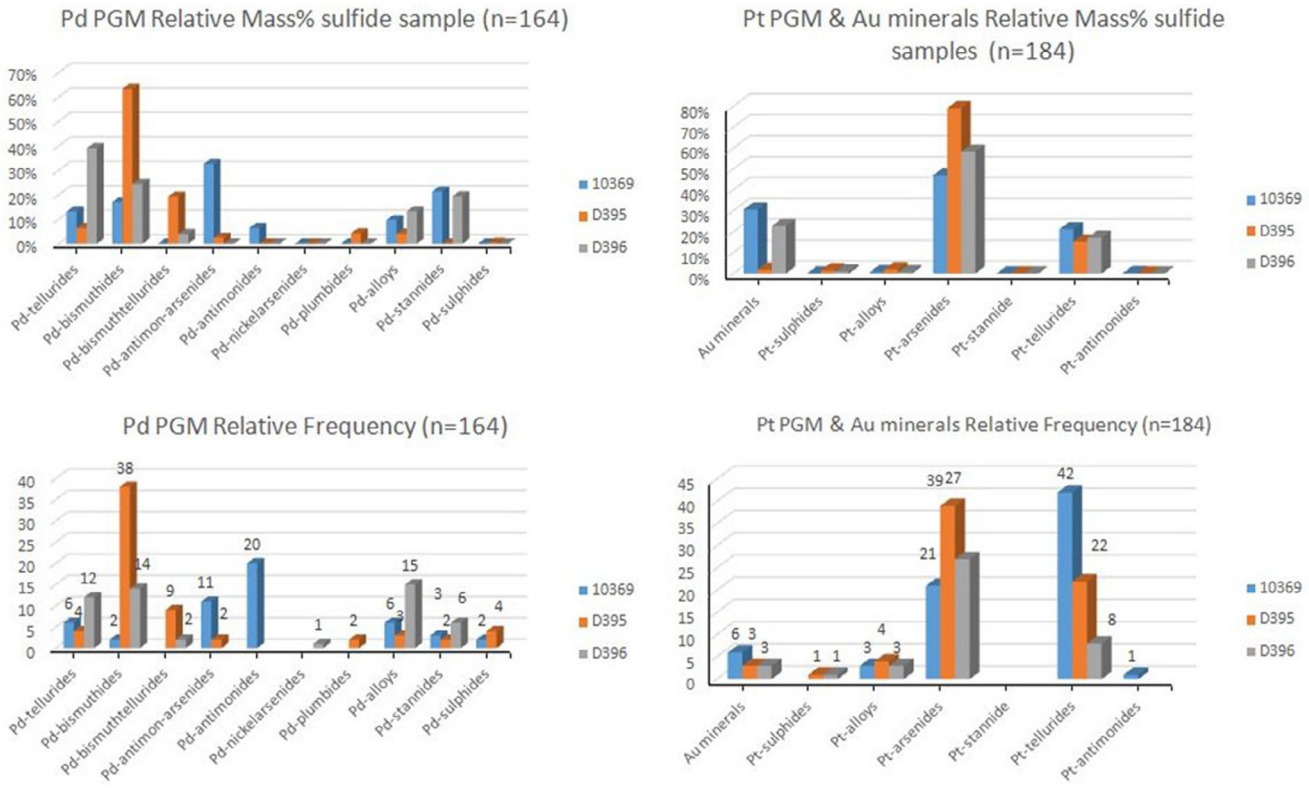

Fig. 8. Relative frequency and mass % of Pd and Pt PGM and gold minerals in three PGE reef samples.

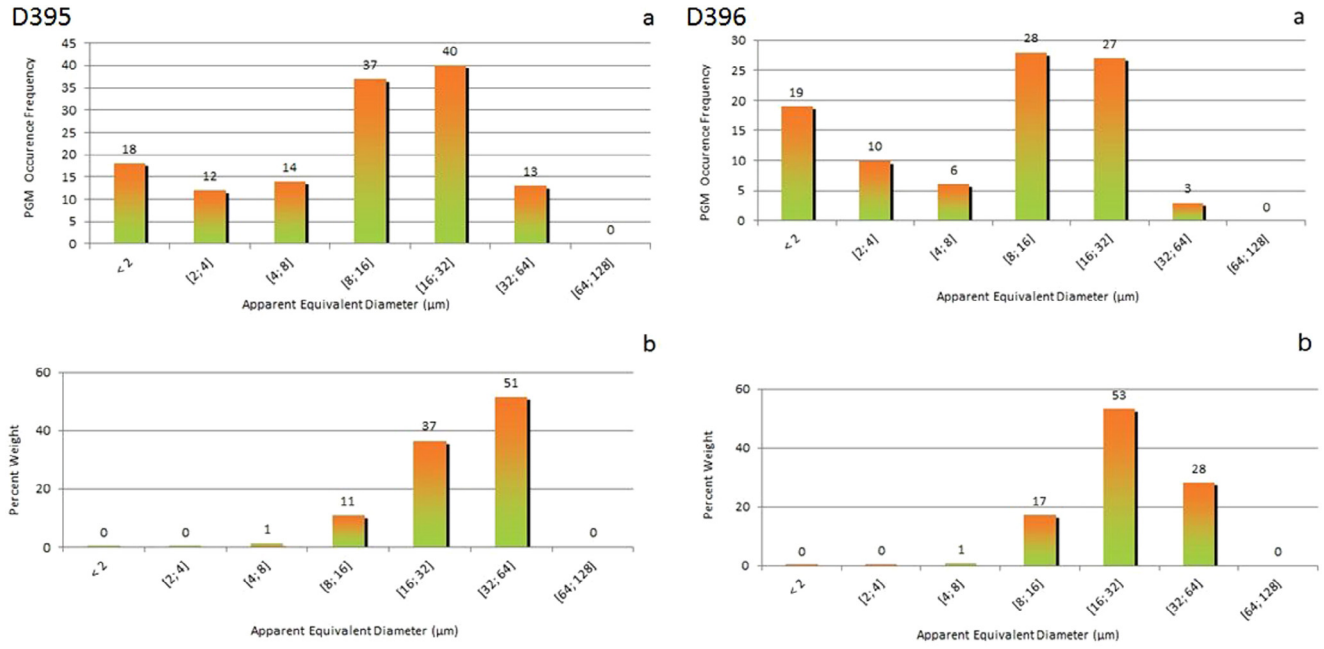

Fig. 9. Grain-size distributions by frequency and mass % of PGM and gold minerals in two PGE reef samples.

increasing in grain-size from ~52 µm to ~70 µm with depth, and (~64 µm in 9550-5, coarser than goethite). Liberation at the optimum grind (K40) for goethite also increases from the top down to 9550-4, ranging from ~43 µm to ~70 µm before becoming ~20 µm in sample 9550-5. Liberation at the optimum grind (K40) for chromite also increases from the top down to sample 9550-4 from ~30 µm to ~53 µm before becoming slightly finer grained in sample 9550-5 (~42 µm). The minimal and optimal grind for chromite and goethite are given in Fig. 12.

7.5. Precious metal mineralogy of the laterite samples

Bulk assays for KPD22 show lowest for Au, Pd, and Pt concentrations in the near surface sample (ferricrete 2.4–5.0 m, 9550-1) and

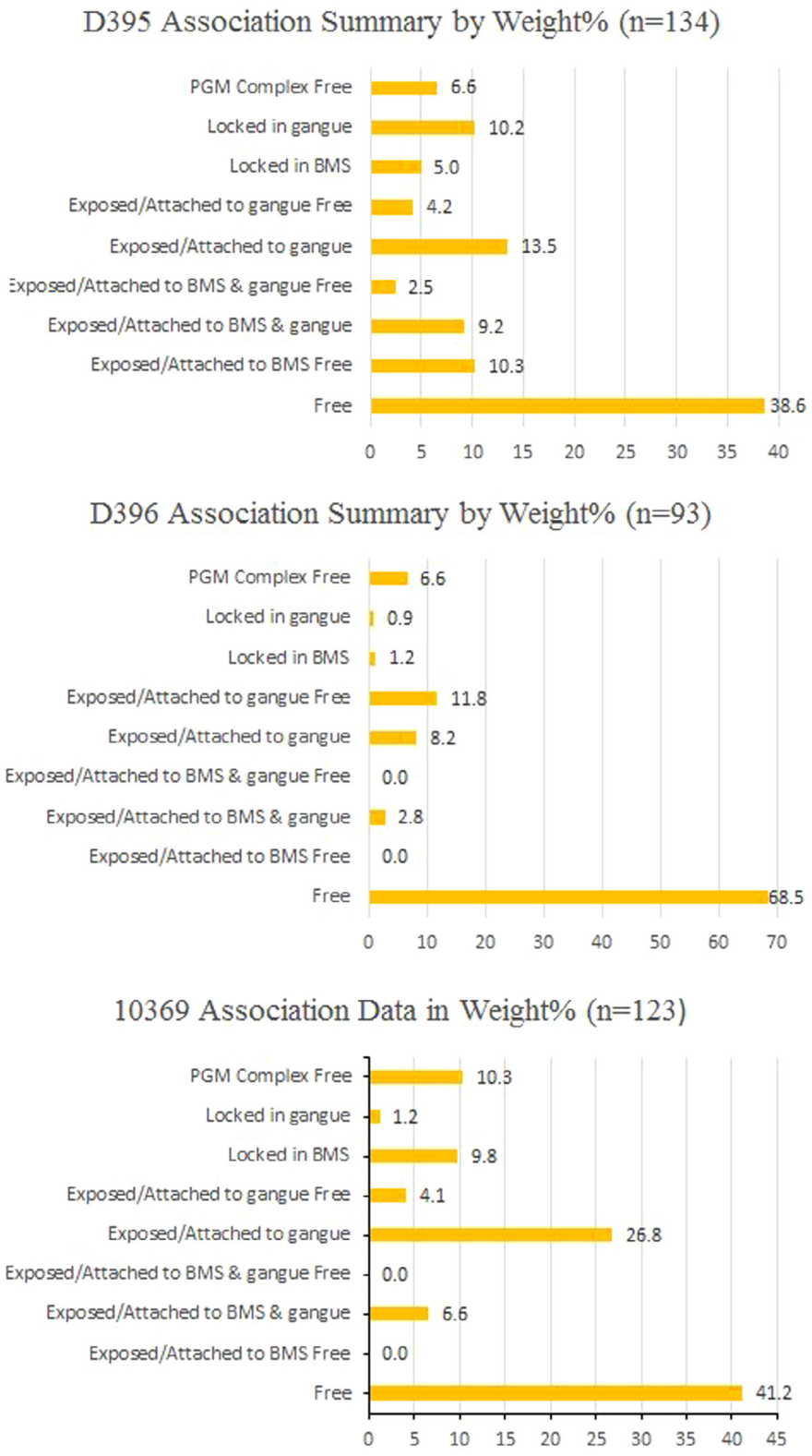

Fig. 10. Association data summary for precious metal minerals in the PGE reef samples.

increase gradually with depth (Fig. 13). In contrast, the proportions between "clay" and "grit" after attritioning varied considerably between the samples from <30% "clay" near surface increasing with depth to ~75% clay. Individual sum and weighted concentrations for (Au, Pd, and Pt) for "clay" and "grit" show contrasting values from near surface (relatively very high values in "clay" fraction) with increased depth. The weighted distributions show an initial drop from near surface (ferricrete 2.4–5.0 m, 9550-1) before gradually increasing from ferralite clay (5.0–7.5 m, 9550-2) to chromite saprolite with depth (13.0–18.5 m, 9550-5).

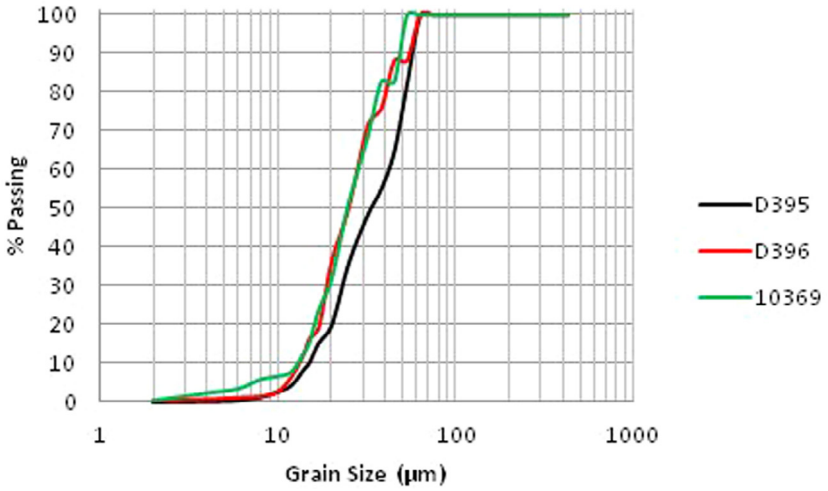

Fig. 11. PGM and Au grain size distributions for three PGE reef samples (n = 364).

Table 4
Measured and calculated modal analyses of five oxidized laterite samples (wt%).

Sample ID: 9550-	1	2	3	4	5
Depth from surface (m)	2.4–5.0	5.0–7.25	7.25–9.5	9.5–13.0	13.0–18.5
Mineral/mineral group					
Gibbsite	0.4	0.4	0.7	0.1	0.7
Halloysite	0.2	0.3	1.7	3.3	5.6
Quartz	4.0	5.7	2.2	2.5	0.4
Talc	0.01	0.01	0.01	0.01	0.02
Clinochlore	0.9	0.4	0.6	2.3	2.1
Goethite	65.2	70.8	74.3	70.3	63.7
Mn-wad	0.7	0.04	0.2	0.3	0.2
Hematite	24.5	7.9	3.9	2.7	3.1
Chromite	4.0	14.5	16.4	18.4	24.2
Zircon	0.04	0.1	0.01	0.05	0.01
Totals	100.0	100.0	100.0	100.0	100.0

Table 5
Measured and calculated chromium and chromite quantities.

Sample ID 9550-	1	2	3	4	5
Depth from surface (m)	2.4–5.0	5.0–7.25	7.25–9.5	9.5–13.0	13.0–18.5
Bulk Cr assay [%]	1.83	3.66	4.92	5.34	7.30
Maximum observed % Cr_2O_3 in chromite	47.95	44.67	56.58	45.91	49.12
Maximum observed % Cr in chromite	32.81	30.56	38.71	31.41	33.61
Average % Cr_2O_3 in chromite	42.56	40.51	44.88	42.88	44.06
Average % Cr in chromite	29.12	27.72	30.71	29.34	30.14
Minimum observed % Cr_2O_3 in chromite	39.17	30.11	41.36	40.94	36.84
Minimum observed % Cr in chromite	26.80	20.60	28.30	28.01	25.21
Amount of chromite from bulk Cr assay and maximum observed Cr in chromite	5.58	11.98	12.71	17.00	21.72
Amount of chromite from bulk Cr assay and average Cr in chromite	**6.28**	**13.21**	**16.02**	**18.20**	**24.22**
Amount of chromite from bulk Cr assay and minimum observed Cr in chromite	6.83	17.77	17.39	19.07	28.96

A total of 139 PGM, gold and silver minerals were found in the five samples, with a variable distribution across the profile as summarized in Wilhelmij and Cabri (2016, Table 4). The PGM are dominantly sperrylite and Pt-Fe alloys with few Pd PGM. No Pt or Pd oxides, such as those in the Main Sulfide Zone (MSZ), Zimbabwe, reported by Evans (2002) and Oberthür et al. (2003), were found. This, together with the paucity of PGM found, especially in the upper group samples (partly because of a combination of low grades and very small available samples for hydroseparation), suggests that a large proportion of the Pt and Pd does not occur as PGM greater that a few micrometers in size or are contained within minerals such as goethite or in a poorly characterized phase referred to as Mn-wad. The precious metal minerals found in the heavy mineral hydroseparation concentrates are shown graphically in Wilhelmij and Cabri (2016, Fig. 13).

7.6. Deportment of nickel in the laterite samples

As recorded in Wilhelmij and Cabri (2016), nickel does not form discrete minerals, with the exception of some rare sulfides (millerite NiS and Pd-bearing heazlewoodite Ni_3S_2), antimony sulfides (ullmannite NiSbS), and sulfarsenides (gersdorffite NiAsS), but occurs in trace amounts in goethite, hematite, and chromite and

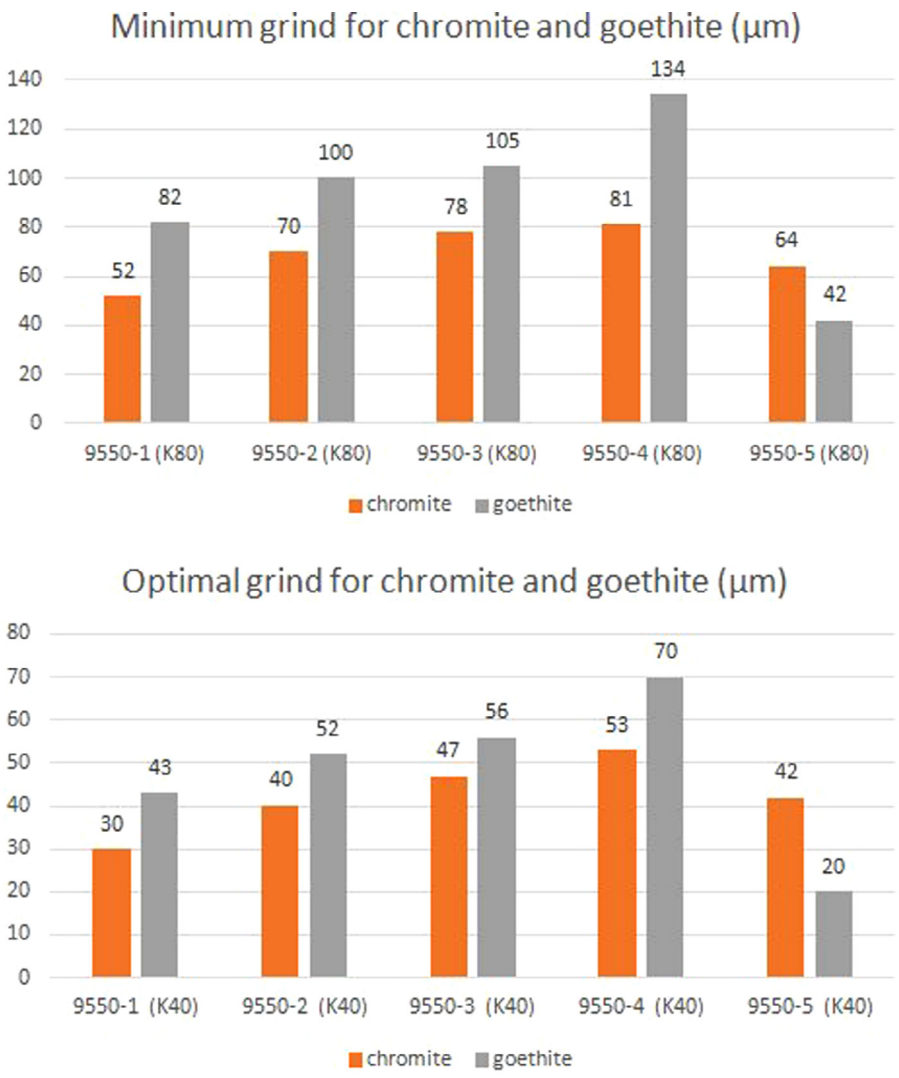

Fig. 12. Minimum (a) & optimum (b) grind for chromite and goethite in the oxidized laterite samples.

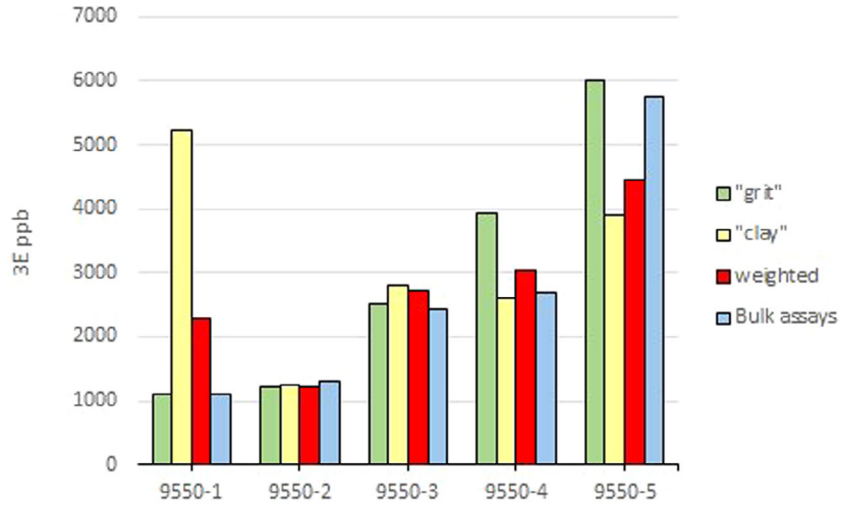

Fig. 13. Relative weighted distributions for Au, Pd and Pt between "grit" and "clay" in the laterite regolith.

about 15–20 wt% NiO occurs in clinochlore and talc. Though clinochlore and talc represent less than 2.5% of the Ni-carriers they are the most significant Ni carriers in the oxidized laterite samples (85.0–97.7%). The Ni contribution from goethite shows a slight progressive increase with depth, as expected, having been formed from pentlandite (Table 6), and is eventually dispersed as indicated

Table 6
Calculated mineralogical deportment of nickel in grit (wt%).

Mineral/sample	9550–1	9550–2	9550–3	9550–4	9550–5
Goethite	0.9%	2.1%	3.8%	5.9%	13.8%
Chromite	0.5%	0.9%	0.7%	0.8%	0.7%
Hematite	0.9%	1.4%	2.6%	1.6%	0.5%
Chlorite + talc	97.7%	95.6%	92.9%	91.8%	85.0%
Totals	100.0%	100.0%	100.0%	100.0%	100.0%

by the progressive decrease in the Ni contribution from clinochlore and talc with depth.

7.7. Metallurgical testwork on Kapalagulu laterite

Five drill core samples were taken from an inclined diamond drill hole (KPD22, location shown in Fig. 2) for PGM analysis and the results are discussed in Wilhelmij and Cabri (2016) and in later sections.

Two vertical large diameter diamond holes (KPD91 and 92) were drilled into the PGE and chromite-rich laterite to take PQ sized core samples for metallurgical testwork. Another four large diameter holes (KPD89, 90, 93 and 94) were drilled into Ni-rich laterite. The six metallurgical drill holes (Table A1) are shown in the stacked cross-sections of Fig. 5 and illustrate the distribution of Cu, Ni, Cr, and Pt + Pd + Au with respect to the various laterite lithologies. Laterite regolith drill core taken from the drill holes was sent to GRD Minproc and Lakefield Ore Test, Perth in Western Australia for metallurgical testwork and the results are discussed in later sections.

GRD Minproc and Lakefield Ore Test in Perth, Western Australia, completed preliminary metallurgical testwork on six different composite laterite samples taken from six strategically-placed vertical metallurgical drill holesKPD89 to KPD94 (Fig. 5), taking into account the mineralogy reported in Cabri (2004c),and geological logging and assaying of the various laterite lithologies (Jones, 2004). These six samples were divided into two groups (Table 7), those containing Ni mineralization with negligible PGE (LoMgSAP, HiMgSAP, SAPRock), and those containing significant PGE (LoMgSAP PGE, HiMgSAP PGE, Ferricrete). Metallurgical testwork focused on the extraction of Ni rather than PGE from the respective composite samples and this work was reviewed by Elias and Wedderburn (2005)

The testwork made recommendations for taking the project forward that related to resource development (e.g., more closely-spaced sampling, documentation, exploration for additional resources) and to process development suggesting that this should focus first on heap leaching, with a fallback to atmospheric leaching. They also recommend that in parallel to this, development work needs to investigate a viable PGE recovery process. Some hydrometallurgical extraction evaluations were performed on the PGE–bearing high magnesium (HiMgSAPPGE) and low magnesium saprolites (LowMgSAPPGE) through the AJ Parker Centre for Integrated Hydrometallurgical Solutions (through its partners Curtin University and CSIRO) and the work was reported by Kasiri (2005). Kasiri evaluated a pressure acid leach (such as used in Nickel Laterites) with the addition of sodium chloride as chloride ligand to form PGE chloride complexes. Although high Pt extractions were obtained, Pd rapidly hydrolyzed causing low to zero extraction of Pd. Kasiri's results are shown in Table 8 below.

Sulfuric acid use was very high (397, 467 and 497 kg_{acid}/t_{ore}). Numerous challenges are evident in these results. The use of acid and chloride ions in an autoclave is extremely aggressive from a materials of construction perspective. The acidic chloride-sulfate mixture will mobilize multiple cations (such as magnesium, aluminum, etc.), although iron is anticipated to remain as hematite as long as temperatures can be maintained above 220 °C. At lower temperatures (below 190 °C) jarosites are expected to form, which may lock up significant precious metals. If the Pd cannot be extracted for this Pd-rich resource, the processing would be hard to justify. Leach residue generation is significant and would require neutralization (with milk-of-lime) prior to further disposal, leading to significant gypsum co-precipitation.

The combination of high acid consumption and associated supply logistics, large quantities of leach residue (and neutralized precipitate) production, and the use of acidic chlorides under pressure-acid leach conditions amount to taking an extreme, but unselective approach (i.e. solubilizing too much gangue).

Other approaches are required and a few are briefly discussed in the following paragraphs. The "Panton Process" developed for the

Table 7
Composite head assays from metallurgical testwork conducted on samples collected from laterite regolith in six diamond drill holes.

Composite Name	SG	Al (%)	Co (ppm)	Cr (%)	Mg (%)	Ni (ppm)	PGE (ppb)
LoMgSAP	3.27	5.67	988	3.83	0.71	9345	N/A
HiMgSAP	2.77	3.82	495	1.87	4.95	12,900	N/A
SAPRock	2.74	2.16	300	1.49	12.1	11,800	N/A
LoMgSAPPGE	3.16	6.77	1420	4.11	0.65	8130	2572
HiMgSAPPGE	2.96	3.72	630	2.54	5.72	13,000	741
Ferricrete	3.22	7.98	193	4.47	0.20	2275	1696

Table 8
Dissolution of Ni, Co and PGE's from Low and High Magnesium Saprolites under pressure acid leaching with different levels of NaCl addition.

Ore sample	NaCl (g/L)	Ni (%)	Co (%)	Pt (%)	Pd (%)	Rh (%)
LowMgSAPPGE	0	95	97	7	0	0
LowMgSAPPGE	10	87	88	76	0	51
LowMgSAPPGE	20	85	85	82	0	60
HiMgSAPPGE	10	98	96	54	0	0
HiMgSAPPGE	20	97	95	70	0	0

high chromite Panton Sill resource in the North of Western Australia (Bax et al., 2009) and discussed by Lewins and Greenaway (2004). This process makes use of a low temperature calcining (400–450 °C) step that makes PGE arsenides (e.g. sperrylite), sulfides and oxy-(hydroxyl) compounds amenable to cyanide leaching. The ore/concentrate is subsequently leached in cyanide and a selective ion exchange to recover base metals and activated carbon as an adsorbent for PGE's. A problem with this approach is the large amounts of cyanide required to solubilize the base metals and the poor recovery of cyanide due to the formation of ferrocyanide, HCN, thiocyanate and cyanate and weak acid dissociable cyanides.

Eksteen et al. (2011) developed a sequential stage heap leach which makes use of an acidic heap bioleach, followed by a solar heated (50–60 °C) cyanide leach to solubilize the PGE's. This approach was found to be successful and solubilized Au and Pd with high leach recoveries, but Pt leaching was limited to a 55–60% extraction after an extended leach. It was noted that the predominant unleached Pt-mineral was sperrylite. The leach kinetics and behavior of Platreef PGM ore and concentrates in such a sequential stage heap leach has been discussed in a number of publications (Mwase et al., 2012a, 2012b, 2014). The recovery by adsorption of the PGM's onto activated carbon from these cyanide based heap leach solutions and the subsequent elution, as well as using a Merrill- Crowe cementation analogue has been reported by Mpinga et al. (2014a, 2014b) and Snyders et al. (2013, 2014, 2015). However, the process was never commercialized or piloted.

Eksteen and Oraby (2014, 2015a, 2015b) have developed a novel alkaline glycine ("GlyLeach") process that does not dissolve iron, magnesium or chromium but is effective to solubilize the chalcophile metals and less reactive siderophile metals (such as Ni, Co) as well as PGE's. The system was shown to have a strong affinity for Pd, Au, Ag and Pt. However, it is anticipated that the process will also be benefitted by a moderate calcining step (400–450 °C) as implemented in the Panton process. If a milling/-grinding process is utilized, early gravity recovery of sperrylite could be considered prior to leaching. One of the major attractions of the process is that the main lixiviant (glycine) is easily recoverable and recyclable, of low cost and is non-toxic. This alkaline process can be operated in the presence or absence of catalytic amounts of cyanide, allowing simultaneous leaching of base metals and precious metals while using minimal concentrations of cyanide, and minimizes the generation of weak acid dissociable cyanides (cyanide complexes of Ni, Cu, Co, including free cyanide and hydrocyanic acid), commonly associated with precious metal bearing ores containing significant Cu, Ni and Co (Oraby and Eksteen, 2014, 2015a, 2015b).

Considering aspects such as leach selectivity, reagent consumption and the generation of hazardous waste products, the more recently developed processes, such as the "Panton Process", Sequential Heap Leach and "GlyLeach" processes, offer significant opportunities to treat these difficult PGE deposits. However, significant process development and piloting would still be required before these processes can be commercialized for deposits such as the Lubalisi Zone PGE mineralized laterite and harzburgite.

8. Discussion and conclusions

8.1. Evaluation of the precious metal mineralogical data

It has been shown that the Pd/Pt ratios calculated from assays were identical or very close to those calculated from the mineralogy (Wilhelmij and Cabri, 2016, Table 5) for the three PGE reef samples, indicating that the relative abundance of Pd and Pt minerals are reliably determined. Comparisons of similar ratios with gold do not compare well, which is not surprising due to the very low gold concentration of the samples (0.14–0.18 g/t). On the other hand, because so much of the Pd in the laterite samples is mineralogically unaccounted for, similar calculations have large errors (Wilhelmij and Cabri, 2016, Table 5). However, the approach used involving attrition milling and hydroseparation of the "grit" fraction resulted in more precious metal minerals (139) than were found. For example, using more traditional methods for larger samples on three different regolith samples (each sample being a composite of an individual laterite horizon) by BGR (Bundesanstalt für Geowissenschaften und Rohstoffe, Hannover). In this case, five precious metal particles were found (two Pt-Fe alloys, silver-poor gold, small gold crystallites on a grain of Fe-Al hydroxide, and one tiny (<1 μm) gold inclusion in a chromite grain in a polished section (Oberthür, 2004, unpublished). One of the Pt-Fe alloys and the gold crystallites on Fe-Al hydroxide are shown in Wilhelmij & Cabri (2016, Fig. 14).

8.2. Comparison of precious metal mineralogy with other deposits

The precious metal minerals found in the PGE reef and laterite are summarized in Fig. 14. In spite of a very large number of articles reporting precious metal minerals, comparison is limited to a few deposits because many articles report qualitative data or species abundance only by frequency percent. Our data on Kapalagulu samples may be simplified to having abundant sperrylite and Pt-Pd tellurides (including bismuthtellurides) as well as sobolevskite, but with sparse Pt-Pd sulfides. We have not found a similar PGM modal mineralogy reported elsewhere, the nearest being reports by Evans et al. (1994), Evans and Spratt (2000), and Oberthür et al. (2013) on the MSZ (Zimbabwe) and on two deposits on the Merensky Reef by Schouwstra et al. (2000) as shown in Table 9.

Comparative data for oxidized mineralization are fewer, but our study of the Kapalagulu laterite may be tentatively compared to weathered/oxidized MSZ since there are no grade recovery curves for the samples (Evans et al., 1994; Evans and Spratt, 2000; Oberthür et al., 2013). However, weathered MSZ is different as it still contains a significant amount of sulfide some of which can be recovered by floatation even though Becker et al. (2014) reported poor recoveries for partially oxidized sulfide minerals, in spite of preconditioning. Comparison may also be made to Becker et al. (2014) who describe metallurgical tests on "silicate reef" ore (comprising the Merensky Reef, Merensky footwall, Upper Pseudo Reef, Pseudo reef and Lower Pseudo Reef) as given in Table 10. The same list of minerals or grouped minerals is used in Tables 9 and 10 to make differences more evident, especially where a species is not reported. It can be seen that different sample trenches can give entirely different precious metal distributions on the weathered MSZ in the reports of Evans et al. (1994) and Evans and Spratt (2000), which in turn are quite different to the summary derived from a much larger data base by Oberthür et al. (2013). Also noteworthy, is that most of the samples of weathered/oxidized MSZ and "silicate reef" still contain relatively abundant Pt-Pd sulfides, whereas none found in the oxidized laterite at Kapalagulu.

8.3. Metallurgical implications of the PGE reef mineralization

The samples in the present study were too small for a completely satisfactory mineralogical characterization so that the data presented should only be considered as a preliminary investigation of the mineralogy. Combined samples D395 and D396 about 90 vol % of the PGM and Au minerals have an ECD coarser than 20 μm, with about 60 vol% coarser than 40 μm. About 57 vol% is either liberated or associated with BMS and hence is recoverable by flotation. Approximately 43 vol% of the PGM and Au minerals are either attached to gangue or attached to gangue and BMS, requir-

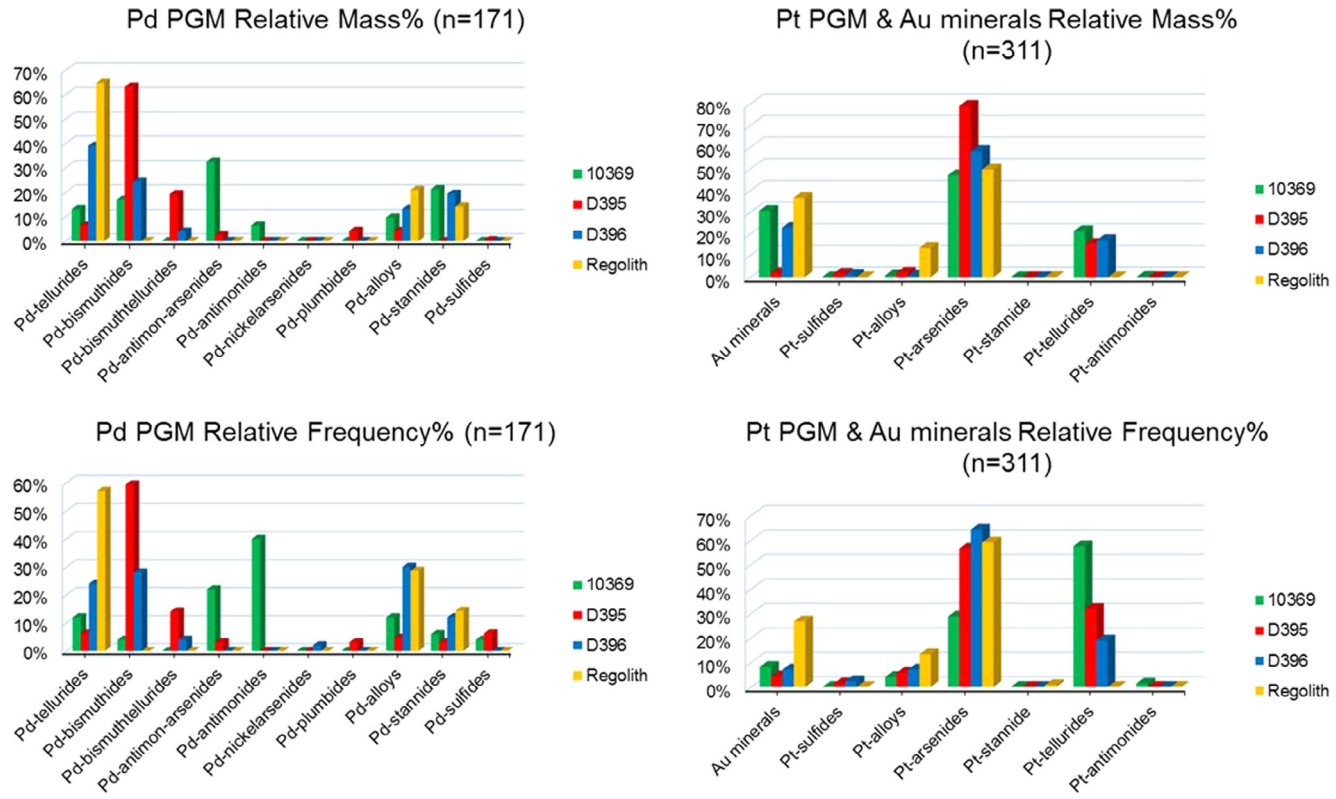

Fig. 14. Pd and Pt + Au minerals comparison between primary and oxidized samples by frequency and mass %.

Table 9
Comparison of precious metal mineralogy in PGE reef samples to other deposits.

	Kapalagulu PGE reef drill core					
	Mass%	Volume%	Mass%	Volume%	Mass%	Volume%
	D395 n = 133		D396 n = 93		10369 n = 123	
Au-Ag	1.1	0.7	15.58	10.6	20.7	16.1
Laurite	–	–	0.09	0.2	–	–
Others	2.9	3.4	7.54	7.6	19.7	20.3
Pd alloys	1.8	1.9	4.58	4.6	3.2	3.3
Pt-Fe alloys	1.1	0.7	0.49	0.6	0.5	0.4
PGE Sulfarsenides	–	–	–	–	–	–
Pt-Pd sulfides	1.1	1.2	0.71	0.8	0	0
Pt-Pd tellurides[1]	19.8	21.3	23.53	25.8	18.6	20.7
Sobolevskite	27.6	25.6	7.57	7.3	5.5	5.3
Sperrylite	44.3	45.1	39.89	42.3	31.8	33.8
	100	100	100	100	100	100

	Evans et al. (1994) D2 drill hole MSZ Mass%	Evans and Spratt (2000) MSZ pristine Mass%		Oberthür et al. (2013) MSZ pristine Frequency%	Schouwstra et al. (2000) Merensky Reef Volume%	
	n = 89	Pt peak n = 181	Pd Peak n = 43	Many studies n = 801	Boschkoppies Many studies	Western Pt Many studies
Au-Ag	5				0.7	4.1
Laurite					8.0	–
Others	2			8.1	Trace	Trace
Pd alloys					2.3	–
Pt-Fe alloys	2	6.5	6.0	2.4	13.1	6.1
PGE Sulfarsenides				11.9		
Pt-Pd sulfides	45	27.0	53.5	8.5	29.4	17.3
Pt-Pd tellurides[1]	43	41.5	37.5	50.1	6.5	21.4
Sobolevskite						
Sperrylite	3	25.0	2.5	19.0	39.9	51.00
	100	100	100	100	100	100

[1] Includes bismuthotellurides.

Table 10
Comparison of precious metal mineralogy in weathered samples to other deposits.

	Evans et al. (1994) Weathered MSZ Trenches 1 & 2	Evans and Spratt (2000) Weathered MSZ Trench		Oberthür et al. (2013) MSZ oxide Many studies	Becker et al. (2014) Weathered "silicate reef"	Kapalagulu Regolith over 18.2 m KPD022	
	Mass%	Mass%	Mass%	Frequency%	Area%	Mass%	Volume%
	n = 31	(Pt peak) n = 88	(Pd peak) n = 80	n = 1293	n = 82	n = 133	
Au-Ag	2.5				0.3	36.1	30.7
Laurite					18.9	–	–
Others				X[1]	21.4[2]	0.5	0.6
Pd alloys	1				30.3	0.2	0.2
Pt-Fe alloys	94			3.1		13.3	9.8
PGE Sulfarsenides				–	2.0	–	–
"Pt-oxide"		56.0	62.0				
Pt-Pd sulfides	2	31.5	33.0	28.3	8.2	–	–
Pt-Pd tellurides[3]		–		11.4	11.6	0.7	0.8
Sobolevskite						–	–
Sperrylite	0.5	12.5	5.0	57.2	7.4	49.1	57.9
	100	100	100	100	100	100	100

[1] No estimate was given for the proportions of (Pt, Pd)-oxides/hydroxides and other PGE-bearing minerals found in the oxidized MSZ.
[2] Others = atokite, arsenopalladinite, plumbopalladinite, sudburyite, "PtPdAs".
[3] Includes bismuthtellurides.

ing some grinding for recovery. The associated sulfide minerals have liberations at minimum grind (K80) of ~25 μm for chalcopyrite, and ~18 μm for pentlandite and pyrrhotite. Because liberation at a minimum grind (K80) is much coarser for chromite (~87 μm), it may be possible to recover the bulk of the chromite at a coarse grind, followed by a finer grind to recover the PGM and sulfide minerals. The PGM, Au and Ag minerals in sample 10369 are finer-grained, with about 25 vol% less than 20 μm ECD, and all are less than 35 μm, without including an electrum outlier. Nearly 70 vol% of the PGM, Au and Ag minerals are liberated, with about 8% associated with BMS. The associated sulfide minerals have liberations at minimum grind (K80) of ~25 μm for chalcopyrite, and ~16 μm for pentlandite and pyrrhotite. Like combined samples D395 and 396, liberation at a minimum grind (K80) is much coarser for chromite (~88 μm), so that it may be possible to recover the bulk of the chromite at a coarse grind, followed by a finer grind to recover the PGM and sulfide minerals.

In summary, there are several challenges to mineral processing and chemical extraction of PGE as the host rocks are relatively fresh and the precious metal mineralization is associated with typical magmatic sulfides with some of the Pd deporting as solid solution in pentlandite. Future detailed mineralogical studies should be undertaken on larger representative or composite samples to confirm the predicted processing route. At the same time, application of trace-element techniques (e.g., Cabri et al., 2008) should be done to constrain the deportment of PGE more closely. It is anticipated that the metallurgical response of the PGE reef ore to conventional grinding and bulk flotation will be good but needs to be confirmed by study of larger samples.

8.4. Evaluation of the laterite mineralization

Our mineralogical investigation did not find any Pt or Pd oxides, such as those reported by Hey (1999), Evans (2002) and Oberthür et al. (2003). This, together with the paucity of PGM found, especially in the upper group samples (because of a combination of low grades and very small sample sizes used for hydroseparation), suggests that a large proportion of the Pt and Pd does not occur as PGM greater that a few micrometers in size. It is obvious that the Pd formerly held in solid solution in pentlandite has now been redistributed, some of which may be held in the goethite that has replaced the sulfide minerals. Oberthür et al. (2003) suggested that the lost Pd and Pt might also be present "...in a dispersed form in iron-oxides/-hydroxides, or in smectites." However, this needs to be confirmed.

The relative paucity and nature of the Pd minerals found in the samples, and when found, these are usually very fine-grained, further suggests that other than some supergene Pd minerals, all the primary Pd mineralization has been dissipated or reconstituted. Some of the dispersed Pd also occurs in remnant supergene heazlewoodite. Some of the primary Pt minerals are more resistant to oxidation and dissolution, especially Pt-Fe alloy and sperrylite. Sperrylite might not be stable in the uppermost sample (9550-1), but occurs in all other samples, whereas minerals such as moncheite are no longer stable and their Pt content is now dispersed. Because sperrylite is so stable, it is possible that it is still present in sample 9550-1, but in the form of very fine particles, though there were no signs of alteration on the sperrylite particles found. However, sperrylite is known to slime easily and its tendency to break down to finer-grained particles even when locked in goethite. Like Pd, one cannot be certain of the present location of the dispersed Pt, but it is likely also associated with goethite, as well as Mn-wad.

Gold, originally occurring as electrum has in some cases now been leached of Ag, to form relatively pure native gold, which was found in all five samples, sometimes together with electrum. A small proportion of the Au has been recrystallized in the form of supergene tetra-auricupride (CuAu), which was found in sample 9550-2. Silver, originally in electrum and in some Ag sulfides and tellurides has recrystallized in the form of native silver in sample 9550-2. Some of the Ag has been recrystallized as a Pd-Ni-Ag mineral in sample 9550-4 and some may be dispersed in some of the gangue minerals.

The relative loss of Pt in the form of PGM to that of Au with depth (or dispersal of gold near surface) may be roughly shown by determining the Pt/Au ratio in the samples from assay values for "grit" (11 for upper two samples to 5.5 for the rest) compared to the ratio determined from the relative weights of Pt and Au calculated from the Pt and Au minerals: ~2 for upper two samples and 0.8 for deeper samples. Whereas the numbers are not very precise, they clearly indicate the trends.

8.5. Metallurgical implications of the laterite mineralization

The assay data for "grit" and "clay", the lack of sulfides, indicate that this mineralization cannot be processed by conven-

Table 11
Chemical characteristics of Kapalagulu laterite to other deposits (Elias and Wedderburn, 2005).

	Mibango (Kapalagulu)		Pinares W	Murrin	Vermelho	Pujada		Ambatovy	Mirabela		
%	LMS	HMS	Limonite	Clay	Average	LMS	HMS	Average	LMS	Clay	HMS
Ni	0.93	1.29	1.06	1.01	0.93	1.24	1.38	1.07	0.71	1.04	1.51
Co	0.10	0.05	0.14	0.06	0.08	0.07	0.05	0.1	0.11	0.06	0.04
MgO	1.2	6.2	1.2	6.1	3.1	1.4	10.6	1.1	1.4	6.7	20
Fe	37	26	47	22	30	34	19	46	41	21	14
SiO_2	11	27	4.6	42	38	17.5	35	10	15	42	39
Al_2O_3	10.7	7.2	7.7	5.1	NA	6.4	3.7	8.3	5.8	3.2	1.5

tional mineral processing techniques. It is likely that a hydrometallurgical route should be investigated to recover the base and precious metals. The oxidized laterite was shown to have several metallurgical domains (Fig. 3) comprising enrichments of Pt, Pd and Au (>1 g/t), Ni (>0.8%), Cu (>0.5%), and Cr (>3%). The scoping study of Elias and Wedderburn (2005) was handicapped as no mineralogical study of the metallurgical test samples was done, thus they assumed the mineralogy to be the same as described in this study for a single drill hole (KPD22). For the metallurgical testwork three samples were selected based on their chemistry: ferricrete, low Mg saprolite (LoMgSAP or LMS), and high Mg saprolite (HiMgSAP or HMS) and they compared some of the chemistry to other deposits (Table 11) using abbreviations of LMS and HMS, respectively, for low and high Mg saprolite for Pinares W (eastern Cuba), Murrin (Western Australia), Vermelho (Brazil), Pujada (Philippines), Ambatovy (Madagascar), and Mirabela (Brazil).

They concluded by suggesting two possible metallurgical options: first option heap leaching and second option atmospheric leaching, for both of which the mineralogy of the feed was required. However, elsewhere in their report they specify that for atmospheric leaching "The key to the process is the use of seawater…", but this seems unlikely for this inland deposit. Other assumptions were a recovery of 50% of contained Pt, Pd, and Au and recovery of Ni and Co. Cu was not considered, nor was it the focus of the mineralogical study, yet a considerable Cu resource is evident. They also comment that "An added benefit of heap leaching is that it is unlikely that the PGE's will dissolve.", but this requires a better understanding of their deportment than is available, especially as the nature of the Pd deportment is not conclusively known. However, acidic chloride based processes are notoriously unselective and significant gangue co-dissolution may result, generating hazardous effluent requiring significant neutralization costs, and heaps with significant rehabilitation costs. The use of an acidic chloride system is therefore not appropriate for this deposit.

For the precious metals there are several direct leach approaches that might be used as discussed in a recent review by Mpinga et al. (2015). This comprehensive review discusses existing technologies in the extractive metallurgy of low-grade refractory precious metals as well as the use of unconventional lixiviants concluding that to date, only four processes (Albion, Nitrogen Species Catalyzed, Outokumpu HydroCopper©, and Total Pressure Oxidation) have been implemented on a large scale for Cu-recovery or for treating precious metal containing feedstocks. Mpinga et al. stress that each deposit has unique precious metal mineralogy, which can be complex, especially in contrast to that of gold. A few processes, such as the "Panton Process", the sequential heap leach process and the "GlyLeach Process" show significant potential for the Kapalagulu deposit, but require significant metallurgical and geometallurgical testing on the ore samples, as well as the piloting of the process at a suitable scale that would allow feasibility studies.

Acknowledgements

We gratefully acknowledge permission to publish by the joint venture partners (Lonmin PLC and Goldstream Mining NL), and also acknowledge the careful work done in different laboratories on behalf of Cabri Consulting Inc: Al Miller (Kishar Research Inc.) for petrography of PTS, Jeanne B. Percival (Geological Survey of Canada) for clay XRD, Rolando Lastra (Canmet) for image analysis and Glenn Poirier for EPMA, and Nikolay V. Rudashevsky (Center for New Technology) for screening, hydroseparation, and SEM analyses and images. LJC is grateful to Megan Becker (University of Cape Town) for providing further details on the "silicate ore" and the authors appreciate discussions and the generosity of Thomas Oberthür (formerly at BGR) in making his unpublished data available. HRW is grateful to Gilberto Fedetto for supervising the drilling of the laterite metallurgical drill holes and for the geological logging of the core and to Martine Wilhelmij for drafting of Figs. 2–5. Finally, the authors are grateful to the reviewers Dave Good, A. S. Macheyeki, and Robert Schouwstra for very helpful reviews, as well as for the comments and guidance of Associate Editor Peter Lightfoot and Editor-in-Chief Franco Pirajno.

Appendix A. Supplementary data

Supplementary data associated with this article can be found, in the online version, at http://dx.doi.org/10.1016/j.oregeorev.2017.04.009.

References

Armstrong, B., 2005. Update to Mibango Resource Estimation Report for Goldstream Mining NL Independent Consulting Report by Black Stump Consulting Group.
Bax, A., Dunn, G.M., Lewins, J.D., 2009. Recovery of platinum group metals. US Patent: US 7,544,231 B2.
Becker, M., Wiese, J., Ramonotsi, M., 2014. Investigation into the mineralogy and flotation performance of oxidised PGM ore. Miner. Eng. 65, 24–32.
Cabri, L.J., 2004a. Petrography and Ore Microscopy of Four Samples From the Kapalagulu Intrusion, Western Tanzania, for Goldstream Mining NL Unpublished Confidential Report 2004-02. 50pp.
Cabri, L.J., 2004b. A Mineralogical Examination of Samples From the Kapalagulu Intrusion, Western Tanzania, for Goldstream Mining NL Unpublished Confidential Report 2004-03, p. 92.
Cabri, L.J., 2004c. Mineralogical Examination of Five Samples From a PGE Regolith, Kapalagulu Intrusion, Tanzania Unpublished Confidential Report 2004-08, p. 92.
Cabri, L.J., 2004d. New developments in process mineralogy of platinum-bearing ores. In: Proceedings Canadian Mineral Processors, 36th Annual Meeting, Ottawa, 189–198.
Cabri, L.J., Beattie, M., Rudashevsky, N.S., Rudashevsky, V.N., 2005. Process mineralogy of Au, Pd and Pt ores from the Skaergaard Intrusion, Greenland, using new technology. Miner. Eng. 18, 887–897.
Cabri, L.J., Rudashevsky, N.S., Rudashevsky, V.N., 2008. Current approaches for the process mineralogy of platinum-group element ores and tailings. In: Ninth International Congress for Applied Mineralogy ICAM 2008. Australian Institute Mining and Metallurgy, Publication Series No 8/2008, pp. 9–17.
Cabri, L.J., McDonald, A.M., Stanley, C.J., Rudashevsky, N.S., Poirier, G., Wilhelmij, H. R., Zhe, W., Rudashevsky, V.N., 2015. Palladosilicide, Pd_2Si, a new mineral from the Kapalagulu Intrusion, Western Tanzania and the Bushveld Complex, South Africa. Mineral. Mag. 79 (2), 295–307.
Cawthorn, R.G., 2002. Platinum-group element deposits in the Bushveld Complex, South Africa. In: Cabri, L.J. (Ed.), The Geology, Geochemistry, Mineralogy and

Mineral Beneficiation of Platinum Group Elements, vol. 54. Canadian Institute Mining Metallurgy Petroleum, Canadian Institute Mining, Quebec, Canada, pp. 389–430.
Cawthorn, R.G., 2015. The Bushveld Complex, South Africa. In: Charlier, B.C., Namur, O., Latypov, R., Tegner, C. (Eds.), Layered Intrusions, pp. 517–588.
Deblond, A., Punzalan, L.E., Boven, A., Tack, L., 2001. The Malagarazi Supergroup of southeast Burundi and its correlative Bukoba Supergroup of northwest Tanzania: neo- and Mesoproterozoic chronostratigraphy constraints from Ar-Ar ages on mafic rocks. J. Afr. Earth Sci. 32, 435–449.
Duchesne, J.-C., Liégeois, J.-P., Deblond, A., Tack, L., 2004. Petrogenesis of the Kabanga-Musongati layered mafic–ultramafic intrusions in Burundi (Kibaran Belt): geochemical, Sr–Nd isotopic constraints and Cr–Ni behavior. J. Afr. Earth Sci. 39, 133–145.
Eksteen, J.J., Oraby, E.A., 2014. A process for precious metals recovery. International Patent Application No.: PCT/AU2014/000877.
Eksteen, J.J., Oraby, E.A., 2015a. Process for selective recovery of chalcophile group elements. International Patent Application No. PCT/AU2016/050171.
Eksteen, J.J., Oraby, E.A., 2015b. The leaching and adsorption of gold using low concentration amino acids and hydrogen peroxide: effect of catalytic ions, sulphide minerals and amino acid type. Miner. Eng. 70, 36–42.
Eksteen, J.J., Petersen, J., Mwase, J.M., 2011. An energy efficient recovery of precious metals and base metals. International Patent Application No. PCT/IB2011/054270.
Elias, M, Wedderburn, B., 2005. Mibango Laterite Nickel Project Scoping Study Project Review Confidential report to Goldstream Mining NL, CSA Australia, p. 33.
Evans, D.M., 2002. Potential for bulk mining of oxidized platinum-group element deposits. Trans. Inst. Min. Metall. 111, B81–B86.
Evans, D.M., Spratt, J., 2000. Platinum and palladium oxides/hydroxides from the Great Dyke, Zimbabwe, and thoughts on their stability and possible extraction. In: Rammlmair et al. (Eds.), Applied Mineralogy. AA Balkema, Rotterdam, pp. 289–292.
Evans, D.M., Buchanan, D.L., Hall, G.E.M., 1994. Dispersion of platinum, palladium and gold from the Main Sulfide Zone, Great Dyke, Zimbabwe. Trans. Inst. Min. Metall. 103, B57–B67.
Evans, D.M., Hunt, J.P.P.M., Simmonds, J.R., 2016. An overview of nickel mineralization in Africa with emphasis on the Mesoproterozoic East African Nickel Belt (EANB). Episodes 39, 319–333.
Gotley, S., 2005. Resource Classification Review for Goldstream Mining NL Lubalisi Nickel Laterite Deposit. Project No 5073: Independent consulting report by Snowden Mining Industry Group Consultants.
Hey, P.J., 1999. The effects of weathering on UG-2 chromitite reef of the Bushveld complex, with special reference to the platinum-group minerals. S. Afr. J. Geol. 102, 251–260.
Jones, G., 2004. Beneficiation, atmospheric leaching and pressure acid leaching of nickel laterite samples from the Mibango Deposit in Tanzania: Lakefield Ore Test Job No 9660.
Kasiri, M., 2005. Investigation of Treatment Options for a Nickel Laterite/Platinum Group Element Ore Unpublished Research report, Curtin University of Technology, p. 63.
Lastra, R., Petruk, W., Wilson, J., 1998. Image analysis techniques and applications to mineral processing. In: Cabri, L.J., Vaughan, D.J. (Eds.), Modern Approaches to Ore and Environmental Mineralogy. Mineral Association Canada, Short Course 27, pp. 327–366.
Lewins, J., Greenaway, T., 2004. The Panton Platinum-Palladium Project. The Australian Institute of Mining and Metallurgy Bulletin, pp. 24–34. July–August, 4.
Maier, W.D., Peltonen, P., Livesey, T., 2007. The ages of the Kabanga North and Kapalagulu intrusions in western Tanzania: a reconnaissance study. Econ. Geol. 102, 147–154.
Maier, W.D., Barnes, S.-J., Bandyayera, D., Livesey, T., Li, C., Ripley, E., 2008. Early Kibaran rift-related mafic–ultramafic magmatism in western Tanzania and Burundi: petrogenesis and ore potential of the Kapalagulu and Musongati layered intrusions. Lithos 101, 24–53.
Mbasha, M.Z., 2007. Geological Characterisation of Nickel and Platinum Group Metals (PGM) Mineralization and Host Rocks at Mibango Project in Rukwa/Kigoma Regions, Western Tanzania (Unpublished MSc dissertation). University of Exeter, p. 101.
Mpinga, C.N., Bradshaw, S.M., Akdogan, G., Snyders, C.A., Eksteen, J.J., 2014a. The extraction of Pt, Pd, and Au from an alkaline cyanide simulated leachate by granular activated carbon. Miner. Eng. 55, 11–17.
Mpinga, C.N., Bradshaw, S.M., Akdogan, G., Snyders, C.A., Eksteen, J.J., 2014b. Evaluation of the Merrill-Crowe process for the simultaneous removal of platinum, palladium and gold from cyanide leach solution. Hydrometallurgy 142, 36–46.
Mpinga, C.N., Eksteen, J.J., Aldrich, C., Dyer, L., 2015. Direct leach approaches to Platinum Group Metal (PGM) ores and concentrates: a review. Miner. Eng. 78, 93–113. http://dx.doi.org/10.1016/j.mineng.2015.04.015.
Mwase, J.M., Petersen, J., Eksteen, J.J., 2012a. A conceptual flowsheet for heap leaching of platinum group metals (PGMs) from a low-grade ore concentrate. Hydrometallurgy 111–112, 129–135.
Mwase, J.M., Petersen, J., Eksteen, J.J., 2012b. Assessing a two stage heap leaching process for Platreef flotation concentrate. Hydrometallurgy 129–130, 74–81.
Mwase, J.M., Petersen, J., Eksteen, J.J., 2014. A novel sequential heap leach process for treating crushed Platreef ore. Hydrometallurgy 141, 97–104.
Oberthür, T., Weiser, T.W., Gast, L., 2003. Geochemistry and mineralogy of platinum-group elements at Hartley Platinum Mine, Zimbabwe. Miner. Deposita 38, 344–355.
Oberthür, T., Melcher, F., Buchholz, P., Locmelis, M., 2013. The oxidized ores of the Main Sulfide Zone, Great Dike, Zimbabwe: turning resources into minable reserves-mineralogy is the key. J. South Afr. Inst. Min. Metall. 113, 191–201.
Oraby, E.A., Eksteen, J.J., 2014. The selective leaching of copper from a gold–copper concentrate in glycine solutions. Hydrometallurgy 50, 14–19.
Oraby, E.A., Eksteen, J.J., 2015a. The leaching and carbon based adsorption behaviour of gold and silver and their alloys in alkaline glycine-peroxide solutions. Hydrometallurgy 152, 199–203.
Oraby, E.A., Eksteen, J.J., 2015b. Gold leaching in cyanide-starved copper solutions in the presence of glycine. Hydrometallurgy 156, 81–88.
Prendergast, M.D., 1988. The geology and economic potential of the PGE-rich Main Sulfide Zone of the Great Dyke, Zimbabwe. In: Prichard et al. (Eds.), Geoplatinum 87. Elsevier, pp. 281–302.
Schouwstra, R.P., Kinloch, E.D., Lee, C.A., 2000. A short geological review of the Bushveld complex. Platin. Met. Rev. 44 (1), 33–39.
Snyders, C.A., Mpinga, C.N., Bradshaw, S.M., Akdogan, G.A., Eksteen, J.J., 2013. The application of activated carbon for the adsorption and elution of platinum group metals from dilute cyanide leach solutions. J. South Afr. Inst. Min. Metall. 113 (5), 389–397.
Snyders, C.A., Bradshaw, S.M., Akdogan, G., Eksteen, J.J., 2014. The effect of temperature, cyanide and base metals on the adsorption of Pt, Pd, and Au onto activated carbon. Hydrometallurgy 149, 132–142.
Snyders, C.A., Bradshaw, S.M., Akdogan, G., Eksteen, J.J., 2015. Factors affecting the elution of Pt, Pd, and Au from activated carbon. Miner. Eng. 80, 14–24.
Van Zyl, C., 1956. The Kapalagulu Basic Complex, Tanganyika Territory (Unpublished MSc thesis). University of Pretoria, p. 54.
Van Zyl, C., 1959. An outline of the geology of the Kapalagulu layered complex, Kungwe Bay, Tanganyika Territory, and aspects of the evolution of layering on basic intrusives. Trans. Geol. Soc. South Afr. LXII, 1–31 (plus two Plates).
Wadsworth, W.J., Dunham, A.C., Almohandis, A.A., 1982. Cryptic variation in the Kapalagulu Layered Intrusion, western Tanzania. Mineral. Mag. 45, 227–236.
Wilhelmij, H.R., Cabri, L.J., 2016. Platinum mineralization in the Kapalagulu intrusion, western Tanzania. Miner. Depos. 51, 343–367. http://dx.doi.org/10.1007/s00126-015-0603-2.
Wilhelmij, H.R., Joseph, G., 2004. Stratigraphic location of platinum mineralisation in the Kapalagulu Intrusion of western Tanzania: Geoscience Africa. In: Ashwal, L.D. (Ed.), Geoscience Africa, vol. 2, pp. 708–709.
Wilhelmij, H.R., Wilhelmij, M.M., 2004. Mibango Project Report on Exploration Kapalagulu Intrusion, May to December 2003 Unpublished Internal Company Report KPP04 for Lonmin – Goldstream JV.
Wilhelmij, H.R., Wilhelmij, M.M., 2005. Mibango Project Report on Exploration Kapalagulu Intrusion, May to December 2004 Unpublished Internal Company Report KPP05 for Lonmin – Goldstream JV.
Wilhelmij, H.R., Wilhelmij, M.M., 2006. Mibango Project Report on Exploration Kapalagulu Intrusion, May to December 2005 Unpublished Internal Company Report KPP06 for Lonmin – Goldstream JV.